PCCP

Accepted Manuscript

ROYAL SOCIETY OF CHEMISTRY

www.rsc.org/pccp

Phys. Chem. Chem. Phys.

Structure and conformational analysis of the anti-HIV reverse transcriptase Inhibitor AZT using MP2 and DFT methods. Differences with the natural nucleoside thymidine. Simulation of the 1st phosphorylation step with ATP

M. ALCOLEA PALAFOX.

Chemical Physics Department, Chemistry Faculty, Complutense University, Ciudad Universitaria, Madrid-28040, SPAIN, alcolea@ucm.es

ABSTRACT

A comprehensive quantum-chemical investigation of the conformational landscape of the nucleoside HIV-1 reverse transcriptase inhibitor AZT (3′-azido-3′deoxythymidine) nucleoside analogue was carried out. The whole conformational parameters (χ, γ, β, δ, ϕ, P, ν_{max}) were analysed as well as the NBO charges. The search located at least 55 stable structures, 9 of which were by MP2 within a 1 kcal/mol electronic energy range of the global minimum. Most conformers were *anti* or *high-anti* around the glycoside bond and with North sugar ring puckering angles. The distribution of all the conformers according to the ranges of stability of the characteristic torsional angles was established. The results obtained were in accordance to those found in related *anti*-HIV nucleoside analogues. The best conformer in the *anti* form corresponded to the calculated values by MP2 of χ = -126.9º, β = 176.4º and γ = 49.1º. An analysis of the lowest vibrations in conformer C1 was carried out. The first hydration shell was simulated and the structural differences with the natural nucleoside deoxythymidine (dT) were determined. The first phosphorylation step was simulated by interacting ATP with the best hydrated clusters of AZT and dT. The Na cations act as a bridge between the phosphate moieties of ATP making easy that $-P3O_3$ receives the H5′ proton from AZT/dT. A proton-transfer mechanism is proposed through the water molecules. When the number of the water molecules surrounding AZT is lower than 8, the first phosphorylation step of AZT can be carried out. However, the appropriate orientation of the O5′-H in dT avoids this limitation and it can be performed with large numbers of water molecules.

Keywords: AZT, azidothymidine, retrovir, zidovudine, anti-HIV, AIDS, antiviral agents, nucleoside reverse transcriptase inhibitors.

1. Introduction

The progress toward the treatment of HIV infections has steadily increased in the past 2 decades.[1,2] Currently, more than 20 drugs have been approved for it.[3-5] Despite significant progress in the design of anti-HIV drugs, many problems remain (i.e. toxicity, strains resistant, low activity, etc). This low activity is due to the 1st phosphorylation step rate limiting reaction, process studied in the present manuscript. In the bibliography many different strategies have been developed in the search for therapeutic agents against AIDS. Most studies have focused on inhibitors of viral reverse transcriptase (RT), a key enzyme in the replicative cycle of HIV, which is an attractive target for chemotherapy.[6] Viral RT is essential for the transcription of viral RNA into proviral DNA in the cytoplasm.[7] Thus, nucleoside analogues play actually a crucial role in the current treatment of cancer and viral infections as the primary components of highly active anti-retroviral therapy (HAART). The most common anti-HIV drug AZT (zidovudine, retrovir) is studied in the present work.

AZT was identified in 1984 as active, first against murine retroviruses and then against HIV in cell culture.[8] In 1987 the Food and Drug Administration (FDA)[9] approved the first antiretroviral therapy with AZT in the infections caused by the Human Immunodeficiency Virus (HIV).[10] AZT is a potent inhibitor of HIV-1 replication and the first clinically successful drug for AIDS and AIDS-related diseases,[11] particularly in combination with other drugs, such as other NRTIs, non-nucleoside transcriptase reverse and protease inhibitors.[4,12] In the host cell, AZT is phosphorylated at the 5′-hydroxyl oxygen atom in three sequential enzymatic steps, and the resulting 5′-triphosphate molecule (AZTTP) competes with the natural substrate, thymidine 5′-triphosphate, for binding to the viral reverse transcriptase enzyme[13]. Finally, viral DNA synthesis is terminated when AZTTP is incorporated in the DNA chain because the 3′ azide (serving as a replacement for a hydroxyl) group prevents further 3′,5′-phosphodiester linkages.[14] In this process, the first phosphorylation step is often the rate limiting reaction, and for this reason, the simulation of this process is the main aim of the present manuscript.

Despite the numerous drawbacks[15,16], AZT remains as one of the key drugs used in the treatment and prevention of HIV infection in both monotherapy and HAART. However, intensive efforts are still needed for the development of novel, more efficacious, and selective nucleoside derivatives,[17] and for this purpose it is useful to establish relationships between structure, conformational features, physicochemical properties and activity of the drugs used today. Different studies have been carried out with this aim in several nucleosides

analogues.[18-22] Thus, the anti-HIV-1 activity appears to depend upon ribose conformation,[23] and differences in this conformation lead to appreciable changes in positions of the thymine ring and of the C5′-OH group. Therefore, and from our understanding, it would be interesting to analyse the different conformational possibilities for AZT, and compare the results with the nucleoside natural thymidine (dT), and with other drugs.

The structural properties of NRTIs, particularly those governed by intramolecular interactions, determine to a great extent their potential therapeutic efficiency. Thus, an accurate knowledge of the flexibility and conformeral properties of a nucleoside would be an important help for the interpretation of drug-target interactions. For instance, efficient phosphorylation depends largely on the spatial structure of the nucleoside, in special the O5′H orientation.[24] Therefore, an extensive conformational analysis identifying all minima on the potential energy surface can be considered as a first step in the design of nucleoside analogues as anti-HIV drugs. For this reason, the conformers of natural nucleosides and nucleoside analogues have been analyzed by different authors.[23,25-34] In earlier works we studied the effect of the hydration on the two most stable conformers of IUdR[20], d4T[24,35] and AZT[36] nucleoside analogues. Now, the present work is devoted to a comprehensive conformational analysis of the nucleoside analogue AZT with full relaxation of all geometric parameters. To our knowledge, AZT has been extensively examined for anti-viral properties[15,16,18,22,23] but less structural and energetic information, obtained from theoretical studies, are available and moreover, they have been calculated at lower level than those shown in the present work.[5,8,18,37-40] The current manuscript completes our extensive investigation of the conformational families of the 2′,3′-didehydro-2′,3′-dideoxy analogues of the canonical nucleosides. The identification of the conformers in the different clusters permits to know how is the molecular structure of AZT that will interact with the corresponding kinase, and through its relative energy value the % population. With acknowledge of the molecular structure of AZT in water solution, can be simulated the 1st phosphorylation step and therefore put light on its mechanism, responsible of the low activity of the nucleosides analogues. If this mechanism is known, as well as the geometry of the nucleosides actives, new antivirus with high activity and low activity can be simulated. In our simulation, the presence of an OH group in position 3′ facilitates the phosphorylation. Other similar groups in this position, instead of the azide group of AZT can also facilitate the phosphorylation.

2. Computational methodology

Calculations were performed using both the MP2 (second-order Møller-Plesset perturbation theory) method, and the B3LYP Density Functional method (DFT). These methods are implemented in the GAUSSIAN 09[41] program package using the Quipu computer of the Computational Center from University Complutense of Madrid. Standard parameters of this package were used under the UNIX version. DFT methods are the most adequate because they provide a compromise between the desired chemical accuracy and heavy demands put on computer time and power. Moreover, DFT methods have been used satisfactory in many studies of nucleoside analogues[24,26-27,35-36,42-44] and drug design.[45] B3LYP was chosen because different studies have shown that the data obtained with it are in good agreement with those obtained by other costly computational methods as MP2, and it predicts vibrational wavenumbers of DNA bases better than HF and MP2 methods.[46-50]

The new M05-2X [51] and M06-L [52] DFT methods were also used. They are members of the M05 and M06 families of density functionals developed by Zhao, Truhlar and Schultz, which were designed to yield broad applicability in chemistry.[53] M05-2X, a meta-hybrid functional, has been shown to yield good results for dispersion-dominated interactions.[54-56] Also M06-L, a local (non-hybrid) meta functional, generally yields good results for a broad range of interactions, including non-covalent interactions.[52-54,56-57] As M06-L is a local functional, it has much reduced cost compared to other meta functionals, and its performance has been tested in the conformation of a peptide.[58]

Several basis set were used starting from 6-31G(d,p) to 6-311++G(3df,pd), but the 6-31G(d,p) represents a compromise between accuracy and computational cost, and thus it was the base set selected as reference for all of the calculations. The aug-cc-pvdz basis set was used with M06-L.

Berny optimisation algorithm was used under the TIGHT convergence criterion. The conformational equilibrium at 298.15 K was evaluated by means of the Boltzmann distribution. 55 optimized geometries were obtained by combining three possible values (g^+, g^- and t) for each of the β, γ and ϕ torsional angles, and three ranges of values for the χ angle (*syn*, *anti*, high-*anti*). Natural NBO procedure was employed for the determination of the atomic charges.[59,60]

Wavenumber calculations were performed on all optimized conformers to confirm the stationary points as local minima on the AZT potential energy landscape and to calculate Gibbs energies ΔG as sum of electronic and thermal free energies. They were carried out at the same level of the respective optimization process and by the analytic evaluation of the second derivative of the energy with respect to nuclear displacement. The absence of imaginary wavenumbers confirmed the optimized conformations to be local minima. Relative energies were obtained by adding zero-point vibrational energies (ZPEs) to the total energy. For the calculation of the ZPEs, the wavenumbers were retained unscaled.

The intramolecular OH···O H-bonds in AZT conformers were determined using geometrical and IR spectral criteria.[25] H-bond energies were evaluated by the empirical logansen's formula.[61]

$$-\Delta H = 0.33\ (\Delta\nu - 40)^{1/2}$$

where ΔH is the H-bond energy in kcal/mol and $\Delta\nu$ is the frequency shift of an H-bonded stretching mode, ν(OH) in cm^{-1}. The shifts of stretching modes were calculated as difference between the average frequencies of all conformers without relevant H-bonds and the frequencies upon H-bonding.

3. Definition of conformational angles

The conformation of a pyrimidinic nucleoside usually involves the determination of seven structural parameters, Scheme 1, which includes the exocyclic and endocyclic torsional angles defined according to Saenger's notation.[62] These are the following: (i) the glycosylic torsional angle χ (O4′-C1′-N1-C2), which determines the three orientations of the pyrimidine base relative to the furanose ring, denoted as *anti*, *high-anti* and *syn*. This torsion angle is intimately related to intramolecular interactions between the sugar and thymine rings. In particular, H-bonding between O2 and H5′ is only possible in *syn* forms. (ii) The exocyclic torsional angle β (H5′-O5′-C5′-C4′), which describes the orientation of the hydroxyl hydrogen H5′. A value of this angle close to 180º facilitates the first phosphorylation step. (iii) The exocyclic torsional angle γ (O5′-C5′-C4′-C3′), which shows the orientation of the O5′ atom related to C3′ of the furanose ring, and it is represented by the three main rotamers namely, γ_{g+}, γ_t, γ_{g-}, or *+sc*, *ap*, *-sc*. (iv) The torsional angle δ (C5′-C4′-C3′-N3′), which describes the orientation of the C5′ atom relative to the furanose ring. (v) The torsional angle ϕ (C2′-C3′-N3′-N3′′), which determines the orientation of the azide moiety relative to the furanose ring. The notation used for this torsional angle is in accordance to several authors,[29,37a-d,40] although it has been also defined[43] with the symbol ε (C4′-C3′-N3′-N3′′). Finally, (vi) the puckering of the furanose ring and its deviation from planarity, which is described by the phase angle of pseudorotation P (0-360º) defined in the bottom of Table 1.

The first step in the conformational analysis of AZT was carried out by plotting 3D Potential Energy Surfaces (PES). These plots were built by rotation of the exocyclic torsional angles χ, β, γ and ϕ, that were simultaneously held fixed at values varying between 0º and 360º in steps of 60º in a first study. All other geometrical parameters were relaxed during these optimisations. Thus, 55 optimized geometries were obtained in this step by minimizing the energy with respect to all geometrical parameters without imposing molecular symmetry constraints, Table 1. In a second step, the dihedral angles were varied in steps of 10º. Thus, the potential energy surface (PES) was accurately obtained as we have carried out on d4T.[19] This surface was used to locate the stable conformers of the molecule.

4. Results and discussion

This section is divided in three parts: the description of the results in the isolated state, the analysis of the hydration shell effects, and the simulation of the 1st phosphorylation step.

4.1 Results in the isolated state

4.1.1 Conformers and energetics

Several earlier works at low computational level have been devoted to the conformational analysis of AZT, mainly at PCILO[37a,37f] and at AM1[8,14,30,40] semiempirical levels. In general, few conformers have been calculated in these references. The optimization of more than 10 conformers has been only reported by AM1 (11 conformers[40], 24 conformers[8], and 70 conformers[14]). It has been established in these works that the preferred glycosidic (χ) angle is *syn*, although the *anti* form appears very close in energy and by Sabio et al[14] it is the global minimum, Table 2. Finally, other authors have optimized only two conformers, but considering them as the most stable in a clear error. E.g. by Hernández et al.[39] the conformers B1 and B5, according to our notation of Table 1, and by Yekeler[18] the conformers B4 (*syn*) and C17 (*anti*). By X-ray[63-66] two conformers (molecules A and B) have been identified in the crystal. The structure corresponds always to *anti* in molecule A and *high-anti* in molecule B, Table 2, and the preferred combination for χ and γ is *anti*-γ_{g+} (molecule A) and *high-anti*- γ_t (molecule B).

Because there are discrepancies in the conformers reported by the different authors, an extensive conformational analysis in the isolated AZT molecule is presented here through a rotation of the exocyclic χ, β, γ, ϕ and δ torsional angles. This study is the most complete reported today at different levels of computation with 55 stables structures obtained. In our calculations, some of the conformers reported by other authors fail to appear as stationary points, and others are found not to be local minima. A detailed collection of the most important conformational parameters of these optimized forms is included in Table 1.

The conformers were classified according to the three ranges of rotation of χ: conformers C (*anti*, -130 ± 15º), conformers A (*high-anti*, -169 ± 10º) and conformers B (*syn*, 70 ± 8º), Fig. 1. The energy criterion was followed for the numbering: firstly, the most stable and also the least active biological forms, conformers B were numbered; Secondly, by analogy to d4T[19,67] and related nucleosides (NSs),[20,35,42-46] the biological active and also found in the crystal, conformers C, and finally those forms only found in the crystal, conformers A. These forms in *high-anti* orientation are energetically the least favourable in the isolated state. The *syn* orientation is not common for A and B DNA strands, but it can be encountered in purine nucleotides involved in left handed (Z-form) helices of RNA and DNA.

Fig. 2 shows the 12 best optimum conformers selected in each range of the rotation angle χ: six of them correspond to conformers C (C1 to C6), three to A (A1 to A3), and three

to B (B1 to B3). The values of the most important structural angles of each conformer are also included in the figure. These conformers might correspond to those observable in the gas phase or in the inert-gas matrixes at low-temperature. At room temperature, according to the Boltzmann distribution and MP2 energy values, 57% of the total population of isolated AZT might correspond to conformers B1-B3, 32% to conformers C1-C5 and 4% to conformer A1. The optimization of these conformers at the B3LYP/6-31G(d,p) and MP2/6-31G(d,p) levels of theory shows only slight geometrical changes, Table 1. This result confirms the relevancy of the DFT B3LYP/6-31G(d,p) level in estimating the geometry of AZT conformers.

Two energy values were considered for each conformer: the electronic energy ΔE + ZPE correction, and the Gibbs energy ΔG, the last two columns of Table 1. The global minimum by MP2 and B3LYP corresponds to the *syn-gg-gg* form with respect to χ, γ and β torsional angles, respectively. By MP2 this conformer is denoted as **B1,** $_4$E, and it appears stabilized by an intramolecular H-bond, Fig. 2. The second most stable form is **B2**, with a molecular structure similar to B**1** except that its azide group is in *trans,* ϕ = 161.9º. The third best conformer corresponds to the *anti* form **C1**.

The calculated conformers of Table 1 differ in general little in energy, appearing all within the electronic energy range ΔE = 0-5.8 kcal/mol, and Gibbs energy range ΔG = 0-5.4 kcal/mol by B3LYP related to the global minimum. This range of values is similar to that found in dT, 0-5.8 kcal/mol, and in d4T,[19] 0-6.2 kcal/mol. However, only eight conformers were found in the range ΔE = 0-2.0 kcal/mol (by criterium of ΔE + ZPE). Among them, conformers C4 with the highest dipole moment (7.85 D by MP2, in B1 is 5.64 D) and C1 (7.70 D) are favoured in a polarisable environment with water. It is noted that by B3LYP the dipole moment is in general underestimated, ca. 0.5-1.0 D as compared to MP2.

From a structural point of view, AZT is very similar to dT, Table 3 and Fig. 1-Sup (Supplementary material). Considering the close conformational similarity between them for the C1 conformer, the different biological activity is presumably due to the presence of the azide group at the 3′ position. This azide group cannot be H-bonded to water molecules and thus open clusters cannot be formed with AZT, but by contrast they are possible with dT making easy the first phosphorylation step.

4.1.2 Conformational angle analysis

The distribution of all the optimized conformers according to their energies, exocyclic torsional angles, and values of P and ν_{max} is shown in Figs. 3-6 and Figs. 2-4Sup. The main

optimum conformers are pointed in these figures. An overall examination of the five exocyclic torsional angles, defining the conformational space of AZT, leads to conclude the following according to B3LYP results:

(i) The interring dihedral angle χ presents a trimodal distribution, conformers A (from –174º to –159º), B (from 61º to 78º) and C (from –144º to –125º), Fig. 4(a) and Fig. 2-Sup(a). Conformers B are the most stable. *Anti* forms (44 conformers A and C) prevail in number over *syn* ones (11 conformers B) and cover a wider range of χ values. Also they dominate in the low energy range < 2 kcal/mol, *anti*/*syn* = 62%/38% by criterium of ΔE + ZPE, and 66%/33% by criterium of ΔG. This fact has been interpreted[25] by the slight less sterical restricted by noncovalent interactions between the base and the sugar residue in the *anti* forms. X-ray[63,65,68-71] and NMR[72] data of AZT and related nucleosides show the χ angle in *anti* orientation, which is the preference for biological activity,[44,73,74] and the usual and expected form to be present in B-DNA.

(ii) β angle has a tetramodal distribution with short range of values: 43º ≤ β_{g+} ≤ 77º (17 conformers), 171º ≤ β_t ≤ 180º (13 conformers), –178º ≤ β_t ≤ -172º (4 conformers), and -91º ≤ β_{g-} ≤ -49º (21 conformers), Fig. 4(b). In these last two ranges appear the less stable conformers, while in the first range appears the most stable ones, Fig. 5 and Fig. 2-Sup(b). The most stable conformer in *anti* orientation, C1, has a β angle of 176º which is appropriate for the first phosphorylation step. However, the value of this angle remarkably changes with the hydration.[36]

(iii) The γ angle has a trimodal distribution falling into three sectors (g^+, g^- and t): the 164º ≤ γ_t ≤ 179º and –177º ≤ γ_t ≤ 171º ranges (18 conformers), the -75º ≤ γ_{g-} ≤ -58º (18 conformers) and 43º ≤ γ_{g+} ≤ 62º (19 conformers), Fig. 4(c). Conformers with γ_{g+} are the most stable, Fig. 5 and Fig. 2-Sup(c). The nine possible combinations of the γ and β torsional angles, which determine the orientation of the methoxy group on the 5′-end of the sugar residue, are observed in the conformational families of the dT derivatives. AZT as other NSs requires a γ+ (or *ap*) conformer for the phosphorylation process, in agreement with theoretical[5] and experimental[90] results.

(iv) δ angle has a bimodal distribution: 75º ≤ δ_{g+} ≤ 114º (37 conformers), and 134º ≤ δ_t ≤ 150º (18 conformers). In dT is 83º ≤ δ_{g+} ≤ 102º and 130º ≤ δ_t ≤ 156º. Some correlation/tendency is observed between δ and P angles, Fig. 4(e).

(v) A trimodal distribution has been obtained for the ϕ angle: 69º ≤ ϕ_{g+} ≤ 113º (26 conformers), 151º ≤ ϕ_t ≤ 175º (16 conformers) and -69º ≤ ϕ_{g-} ≤ -46º (13 conformers), Fig. 4(d). In the two first ranges appear the conformers with the highest stability, while in the last range the conformers are less stable, more than 2 kcal/mol, Fig. 5 and Fig. 2-Sup(d). In dT is mainly 60º ≤ ϕ_{g+} ≤ 70º, 146º ≤ ϕ_t ≤ 178º, -178º ≤ ϕ_t ≤ -172º and -70º ≤ ϕ_{g-} ≤ -54º. Variations in the ϕ angle do not produce significant changes in the conformation adopted by the furanose or by the thymine moiety. Although deviation from the *trans* position has been correlated with an increased C2′-*endo* conformation of the furanose ring.[68] The rotations of the (g^+) azide group in the global minimum-energy structure to produce conformations with g^- and *t* azides states result in energy differences on the order of hydrogen bonding strength.[14] Crystallographic intermolecular forces (including hydrogen bonding) may prevent a g^- azide orientation in the solid state.[14] The azide group of either molecule A or B of the crystal exhibit the same geometry[71] and it is not involved in H-bonding, but it prevents stacks of more than two pyrimidine rings.[66] The azide group is nonlinear with the NNN angle ranges from 171 to 174º, and the N3′′-N3′-C3′-H3′ torsion angle from –37 to –51º. In C1 the NNN angle is 173º in accordance to the crystal.[71] The N′′-N′′′ terminal bond length is nearly 0.1 Å shorter than N′-N′′. This unsymmetrical and very nearly linear arrangement is typical of covalent azido groups. As compared to dT, the azido group in AZT does not cause significant alterations in the conformational preferences of the nucleoside, and mainly changes its polarity and lipophilicity.[37b]

It has been reported[37h] that electron-donating groups at C3′ of dT derivatives would increase the electron density on the C5′-OH group, and thus they would be more suitable for phosphorylation than with an azide group as in AZT.

Correlations among the exocyclic torsional angles γ, χ, ϕ, β and δ were not found, and an almost regular distribution of the conformers can be observed (Figs. 5-6). It can be explained by the high flexibility of the structure, which permits many value combinations of the exocyclic torsional angles.

4.1.3 Thymine moiety

In the analysis of the six most stable conformers, the base heterocycle appears with a very small nonplanarity, in general with torsional angles lower than 2º, unlike the free base[75,76] and the planar uracil molecule,[50] but in accordance to the X-ray data in which the base is planar within 0.01 Å.[71] In general the bond lengths and angles do not differ

significantly of similar NSs. The values of the C-N and C-C single bonds are intermediate between those of the corresponding aromatic and the saturated bonds. Hence, there is some aromatic character on the ring structure. Because of the weak O2···H1′ interaction, the C6-N1-C1′ angle is slight more open than C2-N1-C1′. Their values vary within the 121 to 122º and 116 to 118º limits, respectively. Thus, the deformation angle between the glycosidic N1-C1′ bond and the N1-C2-C6 plane has a significant value, which falls in conformers C into the 3-4º range. In conformer C1 is 3º, and the sum of the dihedral angle on N1 is ca. 360º. The *ipso* angle C2-N1-C6 is the same that in the natural nucleoside dT,[35] 120.9º.

4.1.4 Furanose moiety

The puckering of the furan ring is important mainly in reducing steric interactions and in the spatial relationships among the thymine, hydroxymethyl, and the azide groups. Large puckers result from a rather strong dipole-dipole interaction between the base and the sugar moieties in these conformers. In B1 the furanose moiety appears out-of the thymine ring plane, with a calculated N1-C1′-C2′-C3′ torsional angle of 116°.

The sugar is usually characterized by three structural parameters:[77] (i) the endocyclic torsional angles ν_0 - ν_4; (ii) the pseudorotation phase angle P, Table 1; and (iii) the maximum torsional angle (degree of pucker), ν_{max}. Fig. 3 shows three diagrams with the distribution of all the calculated conformers according to the P angle versus the ΔE, ΔG energies and ν_{max}.

(i) The endocyclic angles have a large range of variability: $-39º \le \nu_o \le 27º$, $-36º \le \nu_1 \le 39º$, $-36º \le \nu_2 \le 39º$, $-38º \le \nu_3 \le 33º$, and $-26º \le \nu_4 \le 39º$. The values of ν_0 to ν_3 angles have in general different sign in conformers A and C. This fact leads to values of the pseudorotation phase angle P in the S-type in conformers C and N-type in conformers A. The algebraic sum of ν_i dihedral angles (i = 0, 1, …,4) is close to 0 for all conformers and fails into the –1.3 to 1.4º range.

(ii) Most conformers are of N-type. In particular 38 conformers are N-type in the range: $3º \le P \le 72º$ ($C_{3'}$-*endo,* $O_{4'}$-*exo*), and 17 conformers are S-type mainly in the range $142º \le P \le 169º$ ($C_{2'}$-*endo*, $C_{1'}$-*exo* symmetrical twist). Conformers *anti* cover the $142º < P < 169º$ and $12º < P < 72º$ ranges, *high-anti* the $150º < P < 152º$ and $3º < P < 33º$ ranges and *syn* the $20º < P < 47º$ range. Few conformers are out of these ranges, and they were not observed in the S/N transition region, P≅270º. Conformers *syn* and *high-anti* favoured N-type, while *anti* favoured mainly S-type.

The relative energies do not vary in a regular manner with respect to the values of P, Fig. 3. In the nine lowest-energy conformers by MP2 (relative energy ≤ 1.0 kcal/mol) six are N-type. Also N-type prevails in the energy range < 2 kcal/mol: S/N = 36%/64%, but in the 2-6 kcal/mol range its number decreases and it is 71%/29%. S-forms rather than the more usual N-forms favour axially oriented 5′-substituents, i.e. the 5′-phosphorylation and anti-HIV activity. This feature is in accordance with our most stable conformer C1 in the *anti* form.

The two most stable conformers in the *anti* form, C1 and C2, differ very small in its energy, 0.063 kcal/mol. However, they have very different values of P, -162.6º and 26.8º, respectively. This feature indicates the flexible nature of AZT and its capacity to adopt different forms of ring pucker depending of the environment.

X-ray reports P values of 171 and 213º respectively for the C3′-exo/C2′-endo and C4′-endo/C3′-exo conformers of AZT,[40,68,71,78] and of 164 and 169º for C2′-endo conformers of 3'-fluoro-3'-deoxythymidine.[79] These values are in accordance to our conformer C1 (P = 163º by MP2). Moreover, the DNA strands contain exclusively the C2′-endo (B-DNA) in accordance to our C1, C4, C5, as well as to other *anti* forms, and the C3′-endo (A-DNA) also in agreement to our C2 as well as to other *anti* forms.

(iii) ν_{max} appears in conformers B in the large range 22º < ν_{max} < 36º, in conformers C 28º < ν_{max} < 39º and in conformers A 32º < ν_{max} < 40º, Fig. 3. The azide group in position g^+ gives rise high values of ν_{max}, 35-40º, i.e. a high flexibility, while in position g^- the values of ν_{max} are slight lower, ca. 26-32º. Taking into account that the value of ν_{max} represents the radius of the pseudorotational cycle, its impact as structural parameters is quite high. An increase in the ring puckering produces an increase in the flexibility of the molecule, which could make easier to adapt to the active site. The average ν_{max} values[80] of the DNA (deoxyribose) and RNA (ribose) sugar moieties are 35º and 37º, respectively, in accordance to conformer C1 (36º by MP2) of AZT, as well as to other conformers of AZT.

4.1.5 Intramolecular H-bonds

The *syn* and *anti* forms of the thymine moiety relative to the furan ring provide opportunities for H-bonding involving O5′-H5′ moiety with either thymine's carbonyl oxygen atom at position 2, its hydrogen atom at position 6, or the O4′ furan ring atom. Several authors have studied the intramolecular H-bonds in related NSs, in special using AIM method,[30-34,77,81,82] and we have consider here its classification according to Desiraju et al.[73,74] In general, five intramolecular H-bonds/interactions may be identified in the main conformers

of AZT: (i) hydroxyl oxygen O5′ and uracil's hydrogen at position 6, O5′···H6,·· (ii) hydroxyl hydrogen H5′ and O4′, (iii) H6 and O4′, O4′···H6, (iv) uracil's carbonyl oxygen atom at position 2 and H1′, O2···H1′, and (v) hydroxyl hydrogen H5′ and O2, O2···H5′.

We are also interested in whether the different intramolecular H-bonds in AZT make significant contributions to its conformational behavior. In this sense, MP2 and DFT calculations and AIM analysis[34] conduct to the same five types of the CH···O H-bonds involving bases and sugar residues, in accordance to our results. The energy values of H-bonds are in the range of 2.3-5.6 kcal mol^{-1}, exceeding the kT value (0.62 kcal mol^{-1}).

Mainly, *anti* forms involve the H-bonds/interactions (i) and (ii), and *high-anti* the (iii) and (iv). By contrast, H-bond (v) occurs only in *syn* forms and *gg-gg* respect to β and γ torsional angles. This H-bond is the strongest one observed in AZT, Fig. 2, and it gives a great stability to the structure of conformers B, especially in B1-B2. Thus, they are the most stable ones. The strength of this H-bond in B conformers is responsible of their large P values among the *syn* forms, as well as β and γ angles smaller in B1-B3 than in the remaining B forms.

H-bond (i) is observed in C1 as well as in the majority of the *anti* conformers with β ca. 180º. It appears to give a moderate stability to the structure. Their values indicate that this H-bond is weak although stronger than (ii) to (iv), and weaker than (v). H-bond/interaction (ii) is in general very weak and it mainly appears in *anti* forms with β ca. ± 60º. H-bond (iii) appears only in *high-anti* forms and it is very weak, as it has been also reported in related NSs.[18] The O4′···H6 distance appears to have some influence in the value of P. Thus, the *high-anti* conformers have the lowest P values. H-bond (iv) appears only in *anti* forms and it is also very weak or even it doesn't exist in the majority of the conformers.

A theoretical analysis of the low-lying vibrations of AZT with frequencies below 200 cm^{-1} was carried out, which indicates a high flexibility in the molecular structure, and in accordance to the low-lying molecular vibrations reported by different authors[83-86].

4.2. Analysis of the first hydration shell of AZT

The discrete method (DM) was used to theoretically simulate the hydration. A sufficient number of explicit water molecules (up to 13) was included surrounding the system, as we have carried out by B3LYP in IUdR[20], d4T[35], 5-FU[87] and AZT[36]. In DM the water molecules provide a description of both the microscopic structure of the solvent and specific solute-solvent interactions. Under this DM, the hydration was carried out following the so-

called modified scheme of monosolvation (MSM), consists of the following steps[88]: first the structure of all possible monohydrated complexes is determined and the complex with the lowest energy is chosen; next, a second water molecule is added and the hydrated complex with the lowest energy is located; this process is repeated until the water molecules form a closed chain around the NS structure. With this procedure, hydrated complexes were obtained that contain the water molecules distributed around the structure.

Clusters with the *syn* and *anti* orientation of χ have been optimized in AZT and dT. The most optimum cluster[36] of AZT with 13 water molecules is *anti* (Fig. 7a) as well as that obtained in dT (Fig. 7b), as compared with those obtained in the *syn* form (Figs. 7c-d), respectively. The difference in energy between the clusters with *anti* and *syn* orientation is 1.94 kcal/mol in AZT vs. 0.68 kcal/mol in dT. This difference is slightly increased considering the Gibbs Free energy, 2.19 in AZT vs. 0.98 kcal/mol in dT. Thus, in solution both AZT and dT are expected to be in a *syn-anti* equilibrium. The cluster determined in AZT appears more compacted with shorter intramolecular distances than that found in dT, Table 4. The water molecules transform conformer C1 to C2, as well as conformer B1 to B2. I.e. the hydration changes the conformers and reduces its number.

Two additional types of clusters were determined in dT, Figs. 7e-f. The cluster of Fig. 7f is the least stable due to the strong variation of the β, γ, and ϕ angles by the attraction of the water molecules that acts as a pincer (printed in the figure) between both OH groups. The orientation of H5′ atom in this cluster (β≈180º) facilitates the first phosphorylation step. Although this cluster is the least stable, however it is the most favourable for the first phosphorylation step, and this kind of cluster is not possible in AZT. Thus, it could be one of the features that lead to a low phosphorylation of AZT. Moreover, the structure of dT appears more open with larger O5′···O4 and O5′···O2 intramolecular distances than that of AZT, and perhaps these distances are the appropriated to interact with the kinase cavity.

When a NS or nucleotide binds to its target enzyme, only one form is expected to be present at the active site.[90] We are in accordance to these authors, and the difference in the molecular structure between the optimum clusters is enough large, that we consider that in solution only one *anti* cluster can enter in the enzyme cavity. Moreover, if the clusters enter in the cavity attracted through N3H and O4 and the hole to enter is something small, the length h (Fig. 7) of *syn* clusters is higher than those *anti*. Thus, although the *syn* clusters appear in higher proportion in solution than the *anti* ones, perhaps they cannot enter in the enzyme cavity and only the *anti* form is phosphorylated.

Several authors have reported[90] the existence of the same invariant conformations in solution and in the solid state by both X-ray and solution NMR studies, however, we are not in accordance with them. The intermolecular H-bonds of the water molecules modify mainly the β and ϕ angles leading to a different global minimum in the isolated state that in solution. Also, the crystal forces and the intermolecular H-bonds with neighbour molecules lead to a different conformation in the solid state that in solution. The hydration also affects remarkably the values of P.

Solution conformation studies by NMR have confirmed that the N and S pseudorotamer populations of the furanose ring of AZT are approximately equal, while Raman spectroscopy[91] suggests that the N form is somewhat predominant.[91] Our calculations corroborate this last feature, with the most stable cluster with C2, as well as the cluster with B2, in N-type. The other calculated clusters in *anti* form are S-type, but they are less stable.

Finally, other feature reported in AZT by NMR is that the π bonds C6=C5 and C4=O are less conjugated in solution than in the solid state.[89] This feature confirms our calculations with larger C=C and C4=O bonds in solution than in the isolated state.

4.3 Simulation of the 1st phosphorylation step

4.3.1 Optimization of the ATP molecule

A full conformational study of this molecule has not been reported yet. Thus, this task was undertaken in similar way as it was carried out in several NSs[19,92,93] and NDs[44,94], but including in this case the M06-L and M05-2X methods. I.e. by plotting the 3D PES through the rotation of the exocyclic torsional angles and the further determination of all the optimum conformers. In the computations ATP was simulated as an anion with -4 negative charge. The global minimum obtained is shown in Fig. 8. In this conformer the triphosphate chain appears over the furanose ring because of strong intramolecular H-bond O2′H···OP3 of 1.5 Å. Another strong intramolecular H-bond appears through O3′-H···O2′. These features reduce the number of conformers in ATP and thus the possible orientations of the triphosphate chain for interactions.

4.3.2 Interaction of AZT with the ATP molecule.

It is often the rate-limiting reaction in the three-step phosphorylation of the NSs analogues in the cavity of the ATP kinases. Thus, it is a crucial step in the activity of these prodrugs, and for this reason the proportion of compound phosphorylated is in general very

small in the majority of the prodrugs. It is so small in d4T[95] and AZT that several authors have report that they are relatively unsusceptible to phosphorylation.

For understanding this first phosphorylation step, in a simplified model was simulated the interaction of ATP with conformers C1 and C3 of AZT, firstly in the isolated state, Fig. 9. The effects of the Na cations on this interaction were secondly determined, Fig. 10. Finally, this ATP interaction was simulated under a hydrated medium, Fig. 11.

4.3.2.1 Simulation in the isolated state.

One possible initial orientation of the -P3O_3 phosphate group of ATP and -CH_2OH group of AZT is shown in Fig. 9a, together with its final optimized form in which two oxygen atoms of -P3O_3 participate in H-bonds with H5′ and H3′ of AZT. The interaction of the phosphate group with the O5′-H moiety of conformer C1 of AZT produces a rotation of the β angle to a value appropriate for phosphorylation (ca. 180º), and as consequence the proton H5′ of AZT, pointed in yellow colour, is transferred to -P3O_3 of ATP. In a new step in the kinase cavity (it is not simulated in the present manuscript) O5′ is bonded to P3 and the P3-OP2 bond is broken, i.e. AZT appears phosphorylated. Similar initial interaction was simulated with dT, Fig. 9b. In the final optimized form both OH groups of dT appear H-bonded to -P3O_3. In this case H5′ is not transferred to the phosphate moiety.

Other initial orientations of ATP and AZT/dT were tested. One of the final optimized structures obtained is when two oxygen atoms of -P3O_3 and one of -P1O_2 participate in intermolecular H-bonds, Fig. 9c. In this structure the hydrogen of the O2′H group of ATP is transferred to P3O_3 instead of the hydrogen of the O5′H group of dT. Thus, this interaction doesn't lead to the proton transfer H5′ to ATP, first step required for the phosphorylation. Another example is the interaction of Fig. 5-Sup, which also doesn´t lead to a proton transfer.

Another optimized interaction is represented in Fig. 9d, which leads with M052X to the stable structure plotted in Fig. 9e. However, this structure is not possible biologically due to two features: O5′H appears oriented to -P2O_3 instead of to -P3O_3, and the proton of O2′H in ATP appears transferred to –P3O_3.

Comparing the interactions of ATP with dT and with AZT, with dT they are stronger than with AZT, and also a new H-bond appears in dT through O3′H. This fact leads to a rotation of the ϕ angle to be in *trans* in dT, but it is not possible in AZT. Perhaps one of these features is responsible of the very different rates of phosphorylation between dT and AZT, and in general among the diverse prodrugs that cause differences in their antiviral activity.

The effects of Na cations on the ATP structure and consequently on its interaction with AZT/dT were analysed. Fig. 10 shows the optimum structure with Na atoms acting as a bridge between the phosphate moieties. This feature impedes the O2′H···OP3 intramolecular H-bond and it leads to a different arrangement of the ATP molecule. Therefore, the proton transfer from O2′-H to $–P3O_3$ of Figs. 9c,e is not possible, and the $-P3O_3$ group appears available to receive H5′ from AZT/dT.

4.3.2.2 Simulation with hydrated clusters.

The first phosphorylation step was simulated including water molecules on AZT/dT. The interaction of ATP with the cluster of dT (Fig. 7f) is shown in Fig. 11a. In this cluster with 13 water molecules, a pincer between O5′H and O3′H groups appears through one water molecule. This fact facilitates the adequate orientation of the H5′ hydrogen to be transferred to $-P3O_3$, and therefore the binding of O5′ to P3. In this last step the enzyme cavity should participate because the final structure obtained in Fig. 11a is stable and the attempts of binding to P3 were not possible.

The interaction of ATP with several hydrated clusters of AZT was simulated. This interaction is not enough strong to rotate the β angle to a value appropriate for phosphorylation ($\beta \approx 180^o$) in the AZT-$(H_2O)_{10}$ cluster of conformer C1. Moreover, the phosphate groups little affect the values of the β and γ torsional angles. This fact indicates that the number of water molecules surrounding the NS in the ATP kinase cavity should be lower than 10. Thus, the interaction of ATP with clusters with lower numbers of water molecules was simulated. As example in Fig. 11b is shown the interaction in the AZT-$(H_2O)_7$ cluster of conformer C3. Similar interaction is observed with the cluster of conformer C1, because the interaction of the phosphate groups is strong enough to rotate the β angle toward the C3 form, which is appropriate for phosphorylation. To be successfully this interaction the orientation of ATP and AZT is very important.

Successive steps in the simulation show that the $-P3O_3$ phosphate group with negative charge takes a proton from a neighbour water molecule. Then, this water molecule in the OH form takes a proton from the C5′-OH group of AZT. Thus, the O5′ atom is high negatively charged and ready to be bonded to the positive P3 atom of ATP. This process involves one water molecule as observed in the cluster with 5 H_2O, or two water molecules as in the cluster with 7 H_2O. This feature indicates that the hydrolysis process of ATP in the phosphorylation implicates a proton transfer between ATP and AZT through the neighbour water molecules.

The interaction of ATP with NS analogues appears more difficult than with the natural NSs. Only when the hydration is simulated with less than 8 water molecules the phosphorylation is possible. I.e. it is the number of water molecules that can be located in the kinase cavity, due to it permits the C5′- OH group rotation to be accessible for -P3O_3 phosphate group. Thus, we can conclude that in the first phosphorylation step by the ATP kinase, the AZT cluster loses some of its water molecules inside of the enzyme cavity facilitating the rotation of C5′-OH bond (β≈180º) and its interaction with the ATP molecule and further phosphorylation. Therefore, the number of water molecules in the cavity surrounding the NS is predicted to be lower than 8.

The interaction of ATP changes the geometry of AZT noticeable (χ= -70.0º, γ = 71.7º, ϕ = -175.8º, P=214.0º) as compared to AZT-$(H_2O)_7$ cluster[36] (χ= -108.9º, γ= 52.1º, P=166.1º), but in both cases the orientation is S-type, i.e. the steps simulated in the first phosphorylation doesn't change the orientation. However, when the phosphate group is bonded to AZT as in AZT 5′-monophosphate (AZTMP, the nikavir molecule[94]) the optimum conformer by B3LYP is N-type (P=78.1º) due to the H-bond –PO_3H···O4′. These results support the NMR studies[89,96] in which AZT 5′-triphosphate (AZTTP) and thymidine 5′-triphosphate (dTTP) bind to reverse transcriptase (RT) in *north*-type with χ in the *anti* range and γ as 60º (+*sc* rotamer). Moreover, the values reported in methano-carba-AZT 5′-triphosphate[90] showed that inhibition of RT occurred almost exclusively with the conformationally locked *north* ($_2$E), which was kinetically indistinguishable from the inhibition produced by AZTTP. The antipodal rigid $_3$E (*south*) conformer, on the other hand, did not inhibit RT.

5. Summary and Conclusions

In the present work we have shown a comprehensive compendium of the possible conformers of AZT molecule. The geometries and values of the properties presented here appear to be the most accurate to date. The most important findings of the present work are the following:

(1) Through a rotation of χ, γ, β, ϕ and δ angles in AZT, the 55 most energetically favourable conformers were identified by MP2 and B3LYP methods. 11 conformers are B (*syn*), 23 conformers are C (*anti*) and 21 conformers are A (*high-anti*). Conformers *syn* and *high-anti* favoured N-type, while conformers *anti* favoured mainly S-type.

(2) The distribution of all the conformers according to the ranges of stability of the characteristic torsional angles was established. The values obtained indicate the flexible

nature of AZT. For a high stability the conformers should have a value of ϕ in the 69º → 113º or 151º → 178º ranges, a value of β in the –91º → -49º or –178º→ -172º ranges, and a value of χ in the 61º → 78º range.

(3) Conformer B1 is the most favourable by ΔE and ΔG energy criterion. However, conformers C are in general more stable than A and B. The H-bond O2···H5′ gives a great stability to conformers B1-B3.

(4) Relationship is not observed between χ and the conformational variables γ, β, ϕ and δ, as well as between γ and ν_{max}. As expected, all these variables are basically independent.

(5) An analysis of the lowest vibrations in conformer C1 has been carried out, and the results compared with those obtained in dT. The different vibrational modes were analysed. The presence of low-lying vibrational modes is indicative of the high conformational flexibility of AZT.

(6) In the isolated state the azido group of AZT does not cause significant change in the molecular structure and conformational preferences as compared to dT. However, in the hydrated form the changes are noticeable. The cluster determined in AZT is more compacted with shorter intramolecular distances than that found in dT. Clusters with β≈180º are not possible in AZT, but they appear feasible in dT.

(7) ATP appears strongly intramolecular H-bonded through the oxygen atoms. Several possible binding of ATP with AZT were analyzed. On the basis of this first phosphorylation step mechanism that we have proposed in a simplified model, the hydrolysis process of ATP by the ATP kinase implicates proton transference between AZT/dT and ATP through the neighbour water molecules.

(8) The effects of the Na cations on the ATP structure were considered. They act as a bridge between the phosphate moieties making easy that the $–P3O_3$ group receives the H5′ proton from AZT/dT.

(9) There is no a single factor primarily responsible for the low phosphorylation of AZT, but the fact that the water molecules cannot be bonded to the azide group makes it difficult to form the pincer between H5′ and H3′, and thus a good orientation of the O5′H group for the phosphorylation.

(10) In our simulation the first phosphorylated step can be carried out when the number of water molecules surrounding AZT is lower than 8, due to the orientation of the H5′ hydrogen (β > 120º) facilitates this phosphorylation step. However, dT has not this limitation due to a pincer through a water molecule can be established between H5′ and

H3′. This feature corroborates the protector effect of the water molecules on the DNA, facilitating the first phosphorylated step with the natural nucleosides, and avoiding or retarding this step with foreign molecules.

(11) The interaction of ATP with the AZT-$(H_2O)_7$ cluster doesn't change the S-type orientation of the furanose ring, but due to the H-bond $–PO_3H\cdots O4'$ in AZTMP it changes to N-type, orientation appropriate to inhibit RT as reported by NMR studies. By the flexible nature of AZT it can adopt a *south* conformation required for phosphorylation and subsequently switch to a *north* form for a better interaction with RT**.**

Acknowledgements

The author wishes to thank to E. Escobar Rivera for the help in the calculations. Also to NILS Science and Sustainability Programme (ES07), 002-ABEL-CM-2014A Call.

Supplementary material available: Figures with the bond lengths and NBO natural atomic charges on the atoms in AZT and dT (Fig. 1-Sup), as well as plots with the distribution of the 55 optimum stable calculated conformers in AZT, according to the values of the exocyclic torsional angles versus the relative energy ΔE, are collected as Figs. 2-4-Sup. Another inadequate ATP-dT interaction is shown in Fig. 5-Sup.

References

[1] A. L. Khandazhinskaya, D.V Yanvarev, M.V. Jasko, A.V. Shipitsin, V.A. Khalizev, S.I. Shram, Y.S. Skoblov, E.A. Shirokova, M.K. Kukhanova, *Drug Metabol. Disposition*, 2009, **37** (3), 494.

[2] C. Charpentier, V. Joly, P. Yeni, F. Brun-Vézinet, *Virologie*, 2013, **17** (3), 182.

[3] (a) E. De Clercq, *Int. J. Antimicrob. Agents*, 2009, **33**, 307. (b) C. A. Taft, C.H.T. de Paula da Silva, *Curr. Comp.-Aided Drug Design*, 2006, **2**, 307. (c) E. De Clercq, *J. Clin. Virol.* 2001, **22**, 73. (d) E. De Clercq, *Biochem. Biophys. Acta*, 2002, **1587**, 258.

[4] E. De Clercq, Reverse transcriptase inhibitors as anti-HIV drugs. In: Antiviral Against AIDS, R.E. Unger, J. Kreuter, H. Rübsamen-Waigmann, Eds., Marcel Dekker, Inc., New York, 2000, 107.

[5] M. Arissawa, C. A. Taft, J. Felcman, *Int. J. Quantum Chem*., 2003, **93**, 422.

[6] K. Das, E. Arnold, *Curr. Opinion Virology*, 2013, **3**, 111 & 119

[7] K. Parang, L.I. Wiebe, E.E. Knaus, *Curr. Med. Chem.,* 2000, **7**, 995.

[8] G. M. Ciuffo, M. B. Santillan, M. R. Estrada, L. J. Yamin, E. A. Jáuregui, *J. Mol. Struct. (Theochem),* 1998, **428**, 155.

[9] Food and Drug Administration (FDA). http://www.fda.gov.

[10] (a) L. K. Naeger, N. A. Margot, M. D. Miller, *Antimicrob. Agents & Chemother.,* 2002, **46** (7), 2179. (b) S. Pornprasert, J.-Y. Mary, A. Faye, P. Leechanachai, A. Limtrakul, S. Rugpao, P. Sirivatanapa, V. Gomuthbutra, W. Matanasaravoot, S. Le Coeur, M. Lallemant, F. Barré-Sinoussi, E. Menu, N. Ngo-Giang-Huong, *Curr. HIV Res*., 2009, **7** (2), 211. (c) A. Violari, M. F. Cotton, D. M. Gibb, A. G. Babiker, J. Steyn, S. A. Madhi, P. Jean-Philippe, J. A. Mcintyre, *New England J. Med*. 2008, **359** (21), 2233. (d) R. A. Seaton, R. Fox, N. Bodasing, S. E. Peters, Y. Gourlay, *Aids* 2003, **17** (3), 445.

[11] (a) M.A. Fischl, D.D. Richman, M.H. Grieco, M.S. Gottlieb, P.A. Volberding, O.L. Laskin, J.M. Leedom, J.E. Groopman, D. Mildvan, R.T. Schooley, G.G. Jackson, D.T. Durack, D. King, *N. Engl. J. Med.*, 1987, **317**, 185. (b) H. Mitsuya, K.J. Weinhold, P.A. Furman, M.H. St Clair, S.N. Lehrman, R.C. Gallo, D. Bolognesi, D.W. Barry, S. Broder, *Proc. Natl. Acad. Sci. U.S.A*., 1985, **82**, 7096.

[12] L. Taisheng, G. Fuping, L. Yijia, Z. Chengda, H. Yang, L. Wei, H. Yun, L. Hongzhou, X. Jing, H. Aiqiong, L. Yanling, T. Xiaoping, W. Hui, Z. Tong, G. Guiju, L. Junkang, Z. Xiaoying, W. Xinhua, S. Yongtao, B. Jinsong, L. Ling, W. Huanling, *Chinese Med. J.,* 2014, **127** (1), 59.

[13] (a) V. K. Tandon, R. B. Chhor, *Curr. Med. Chem.: Anti-Infective Agents* 2005, **4** (1), 3. (b) J.-L. Fang, L. J. McGarrity, F. A. Beland, *Mutagenesis*, 2009, **24** (2), 133.

[14] M. Sabio, S. Topiol, *J. Comp. Chem.* 1992, **13** (4), 478.

[15] C. Tortorella, D. Guidolin, L. Petrelli, R. De Toni, O. Milanesi, E. Ruga, P. Rebuffat, S. Bova, *Int. J. Molec. Med*., 2009, **23** (6), 799.

[16] E.R. Kline, L. Bassit, B. I. Hernandez-Santiago, M. A. Detorio, B. Liang, D. J. Kleinhenz, E. R. Walp, S. Dikalov, D. P. Jones, R. F. Schinazi, R. L. Sutliff, *Cardiovasc. Toxicol*., 2009, **9** (1), 1.

[17] V. R. Sirivolu, S. K. V. Vernekar, T. Ilina, N. S. Myshakina, M. A. Parniak, Z. Wang, *J. Med. Chem.,* 2013, **56**, 8765.

[18] (a) H. Yekeler, *J. Mol. Struct. (Theochem),* 2004, **684**, 223. (b) U. D. Bayraktar, L. A. Diaz, B. Ashlock, et al. *Leukemia Lymphoma*, 2014, **55** (4), 786. (c) L. Hansen, I. Parker, L. M. Roberts, et al., *J. Biomechan.,* 2013, **46** (9), 1540.

[19] M. Alcolea Palafox, N. Iza, *J. Molec. Struct*., 2012, **1028**, 181.

[20] M. Alcolea Palafox, *Struct. Chem*., 2014, **25**, 53.

[21] M.C. Alvarez-Ros, M. Alcolea Palafox, *Pharmaceuticals,* 2014**, 7**, 695.

[22] (a) N.A. Al-Masoudi, Y.A. Al-Soud, I.A.I. Ali, T. Schuppler, Ch. Pannecouque, E. De Clercq, *Nucleos. Nucleot. Nucleic Acids*, 2007, **26**, 223. (b) Y. Sato, K. Utsumi, T. Maruyama, T. Kimura, I. Yamamoto, D.D. Richman, *Chem. Pharm. Bull*, 1994, **42**, 595.

[23] P. Van Roey, E. W. Taylor, C. K. Chu, R. F. Schinazi, *J. Am. Chem. Soc.,* 1993, **115**, 5365.

[24] M. Alcolea Palafox, N. Iza, *Phys. Chem. Chem. Phys*., 2010, **12**, 881.

[25] Y.P. Yurenko, R.O. Zhurakivsky, M. Ghomi, S.P. Samijlenko, D.M. Hovorun, *J. Phys. Chem. B* 2007, **111**, 9655.

[26] Y.P. Yurenko, R.O. Zhurakivsky, M. Ghomi, S.P. Samijlenko, D.M. Hovorun, *J. Phys. Chem. B* 2008, **112**, 1240.

[27] Y.P. Yurenko, R.O. Zhurakivsky, M. Ghomi, S.P. Samijlenko, D.M. Hovorun, *J. Phys. Chem. B* 2007, **111**, 6263. (b) A.G. Ponomareva, Y.P. Yurenko, R.O. Zhurakivsky, T. van Mourik and D.

M. Hovorun, *J. Biomolec. Struct. Dyn.,* 2014, DOI:10.1080/07391102.2013.789401. (c) A.G. Ponomareva, Y.P. Yurenko, R.O. Zhurakivsky, T. van Mourik and D. M. Hovorun, *Phys. Chem. Chem. Phys*., 2012, **14**, 6787. (d) A.G. Ponomareva, Y.P. Yurenko, R.O. Zhurakivsky, T. van Mourik and D. M. Hovorun, *Current Phys. Chem*., 2013, **3**, 83.

[28] O.V. Shishkin, A. Pelmenschikov, D.M. Hovorun, J. Leszczynski, *J. Molec. Struct*., 2000, **526**, 329.

[29] M.T. Baumgartner, M.I. Motura, R.H. Contreras, A.B. Pierini, M.C. Briñón. *Nucleos. Nucleot. Nucleic Acids*, 2003, **22** (1), 45.

[30] O.O. Brovarets', Y.P. Yurenko, I.Y. Dubey, D.M. Hovorun, *J. Biomol. Struct. Dyn.,* 2012, **29***,* 1101.

[31] O.O. Brovarets', D.M. Hovorun, *J. Biomol. Struct. Dyn*., 2014, **32**, 127.

[32] O.O. Brovarets', D.M. Hovorun, *J. Biomol. Struct. Dyn.,* 2013, **31**, 913.

[33] T.Y. Nikolaienko, L.A. Bulavin, D.M. Hovorun, *J. Biomol. Struct. Dyn.,* 2011, **29**, 563.

[34] Y.P. Yurenko, R.O. Zhurakivsky, S.P. Samijlenko, D.M. Hovorun, *J. Biomol. Struct. Dyn.*, 2011, **29** (1), 51.

[35] M. Alcolea Palafox, N. Iza, M. de la Fuente, R. Navarro, *J. Phys. Chem.* B, 2009, **113** (8), 2458.

[36] M. Alcolea Palafox, J. Talaya, *J. Phys. Chem*. B, 2010, **114**, 15199.

[37] (a) A. Saran, R. P. Ojha, *J. Biosci*. 1991, **16** (1-2), 29. (b) I. Novak, B. Kovac, *J. Org. Chem*. 2003, **68** (14), 5777. (c) V. O. Nava-Salgado, R. Martínez, M. F. R. Arroyo, G. R. Galicia, *J. Mol. Struct. (Theochem),* 2000, **504**, 69. (d) M. Monajjemi, A. Abedi, H. Passdar, *Bull. Chem. Soc. Ethiop,* 2006, **20** (1), 133. (e) M.T. Baumgartner, M.I. Motura, R.H. Contreras, A.B. Pierini, M.C. Briñón, *Nucleos. Nucleot. Nucleic Acids,* 2003, **22** (1), 45. (f) A. Saran, R. P. Ojha, *J. Mol. Struct. (Theochem),* 1993, **284**, 223. (g) M. Arissawa, J. Felcman, J.O.M. Herrera, *J. Biochem. Molec. Bio*., 2003, **36** (3), 243. (h) A.H. Essa, M. Ibrahim, A.J. Hameed, N.A. Al-Masoudi, *Arkivoc,* 2008, **xiii**, 255.

[38] H. Xinjuan, H. Mingbao, Y. Dayu, *Sci. China, Series B,* 2002, **45** (5), 470.

[39] J. Hernández, H. Soscún, A. Hinchliffe, *Internet Electronic J. Mol. Design,* 2003**, 2**, 589.

[40] C.M. Estévez, A. M. Graña, M.A. Ríos, *J. Mol. Struct. (Theochem),* 1993, **288**, 207.

[41] Gaussian 09, Revision D.01, M. J. Frisch, G. W. Trucks, H. B. Schlegel, G. E. Scuseria, M. A. Robb, J. R. Cheeseman, G. Scalmani, V. Barone, B. Mennucci, G. A. Petersson, H. Nakatsuji, M. Caricato, X. Li, H. P. Hratchian, A. F. Izmaylov, J. Bloino, G. Zheng, J. L. Sonnenberg, M. Hada, M. Ehara, K. Toyota, R. Fukuda, J. Hasegawa, M. Ishida, T. Nakajima, Y. Honda, O. Kitao, H. Nakai, T. Vreven, J. A. Montgomery, Jr., J. E. Peralta, F. Ogliaro, M. Bearpark, J. J. Heyd, E. Brothers, K. N. Kudin, V. N. Staroverov, R. Kobayashi, J. Normand, K. Raghavachari, A. Rendell, J. C. Burant, S. S. Iyengar, J. Tomasi, M. Cossi, N. Rega, J. M. Millam, M. Klene, J. E. Knox, J. B. Cross, V. Bakken, C. Adamo, J. Jaramillo, R. Gomperts, R. E. Stratmann, O. Yazyev, A. J. Austin, R. Cammi, C. Pomelli, J. W. Ochterski, R. L. Martin, K. Morokuma, V. G. Zakrzewski, G. A. Voth, P. Salvador, J. J. Dannenberg, S. Dapprich, A. D. Daniels, Ö. Farkas, J. B. Foresman, J. V. Ortiz, J. Cioslowski, and D. J. Fox, Gaussian, Inc., Wallingford CT, 2009.

[42] M. Hoffmann, J. Rychlewski, *Rev. Mod. Quant. Chem*., 2002, **2,** 1767.

[43] O.V. Shishkin, L. Gorb, J. Leszczynski, *Int. J. Mol. Sci.,* 2000, **1,** 17.

[44] A. Tamara Molina, M. Alcolea Palafox, *Chem. Phys.,* 2011, **387**, 11.

[45] M. Alcolea Palafox, P. Posada-Moreno, A.L. Villarino-Marín, C. Martinez-Rincon, I. Ortuño-Soriano, I. Zaragoza-García, *J. Comp. Aided Molec. Design*, 2011, **25**, 145.

[46] M. Alcolea Palafox, O.F. Nielsen, K. Lang, P. Garg, V.K. Rastogi, *Asian Chem. Letts.,* 2004, **8** 81.

[47] M. Alcolea Palafox, V.K. Rastogi, *Spectrochim. Acta* A, 2002, **58**, 411.

[48] M. Alcolea Palafox, Recent Res. Devel. in Physical Chem. Transworld Research Network, India, 1998, *2*.

[49] M. Alcolea Palafox, *Int. J. Quantum Chem.* 2000, **77**, 661.

[50] M. Alcolea Palafox, N. Iza, M. Gil, *J. Molec. Struct. (Theochem),* 2002, **585**, 69.

[51] Y. Zhao, N.E. Schultz, D.G. Truhlar, *J. Chem. Theor. Comput.,* 2006, **2**, 364.

[52] Y. Zhao, D.G. Truhlar, *J. Chem. Phys.*, 2006, **125**, 194101.

[53] Y. Zhao, D.G. Truhlar, *Chem. Phys. Letts.*, 2011, **502**, 1.

[54] H.R. Leverentz, D.G. Truhlar, *J. Phys. Chem.* A, 2008, **112**, 6009.

[55] T. van Mourik, *J. Chem. Theor. Comput*., 2008, **4**, 1610.

[56] Y. Zhao, D.G. Truhlar, *Acc. Chem. Res*., 2008, **41**, 157.
[57] D. Benitez, E. Tkatchouk, I.I. Yoon, *J. Am. Chem. Soc.*, 2008, **130**, 14928
[58] J. Cao, T. van Mourik, *Chem. Phys. Letts.*, 2010, **485**, 40.
[59] J.E. Carpenter, F. Weinhold, *J. Molec. Struct. (Theochem),* 1988, **169**, 41.
[60] A.E. Reed, L.A. Curtiss, F. Weinhold, *Chem. Rev.,* 1988, **88**, 899.
[61] A. V. Logansen, (1981). *Hydrogen bond (Russian)*, p. 112. Nauka, Moscow
[62] W. Saenger, In Principles in Nucleic Acid Structure, Springer Verlag: New York, 1984, p. 88.
[63] G.I. Birnbaum, J. Giziewicz, E.J. Gabe, T.-S. Lin, W.H. Prusoff, *Can. J. Chem.*, 1987, **65**, 2135.
[64] P. Van Roey, J.M. Salerno, W.L. Duax, C.K. Chu, M.K. Ahn, R.F. Schinazi, *J. Am. Chem. Soc.* 1988, **110**, 2277.
[65] I. Dyer, J.N. Low, P. Tollin, H.R. Wilson, R. A. Howie, *Acta Cryst.,* 1988, **C44**, 767.
[66] R. Parthasarathy, H. Kim, *Biochem. Biophys. Res. Commun*., 1988, **152**, 351.
[67] M. Alcolea Palafox, N. Iza, *Struct. Chem*., 2013, **24**, 967.
[68] P. Van Roey, J.M. Salerno, C.K. Chu, R.F. Schinazi, *Proc. Natl. Acad. Sci. USA,* 1989, **86**, 3929.
[69] G.V. Gurskaya, E.N. Tsapkina, N.V. Skaptsova, A.A. Kraevskii, S.V. Lindeman, Y.T. Struchkov, *Dokl. Akad. Nauk. SSSR,* 1986, **291**, 854.
[70] T.K. Parthasara, *Biochem. Biophys. Res. Commun.*, 1988, **152**, 351.
[71] A. Carmerman, D. Mastropaolo, N. Camerman, *Proc. Natl. Acad. Sci. USA,* 1987, **84**, 8239.
[72] G.V.T. Swapna, B. Jgannadh, M.K. Gurjar, A.C. Kunwar, *Biochem. Biophys. Res. Commun.,* 1989, **164** (3), 1086.
[73] G.R. Desiraju, T. Steiner, The Weak Hydrogen Bond; Oxford University Press, New York, 1999.
[74] S.K. Panigrahi, G.R. Desiraju, *J. Biosci.*, 2007, **32** (4), 677.
[75] P. Hobza, J. Šponer, *Chem. Rev.*, 1999, **99**, 3247.
[76] V.K. Rastogi, C. Singh, V. Jain, M. Alcolea Palafox, *J. Raman Spectrosc.*, 2000, **31**, 1005.
[77] N.G. Fidanza, G.L. Sosa, R.M. Lobayan, N.M. Peruchena, *J. Molec. Struct. (Theochem),* 2005, **722**, 65.
[78] Y. Cheng, G.E. Dutschman, K.F. Bastow, M.G. Sarngadharan, R.Y.C. Ting, *J. Biol. Chem.,* 1987, **262** (5), 2187.
[79] N. Camerman, D. Mastropaolo, A. Camerman, *Proc. Natl. Acad. Sci. USA*, 1990, **87**, 3534.
[80] A. Gelbin, B. Schneider, L. Clowney, S.-H. Hsieh, W. K. Olson, H. M. Berman, *J. Am. Chem. Soc.*, 1996, **118**, 519.
[81] Y.R. Mishchuk, A.L. Potyagaylo, D.M. Hovorun, *J. Molec. Struct.,* 2000, **552**, 283.
[82] Y.P. Yurenko, R.O. Zhurakivsky, S.P. Samijlenko, M. Ghomi, D.M. Hovorun, *Chem. Phys. Letts.,* 2007, **447**, 140.
[83] O. V. Shishkin, A. Pelmenschikov, D. M. Hovorun, J. Leszczynski, *Chem. Phys.*, 2000, **260**, 317.
[84] (a) D. M. Hovorun, Ya. R. Mishchuk, Ye. P. Yurenko, *Biopolymer Cell*, 2002, **18** (3), 219. (b) P. Martel, B. Hennion, D. Durand, P. Calmettes, *J. Biomol. Struct. Dyn.*, 1994, **12** (2), 401.
[85] A. Pelmenschikov, D. M. Hovorun, O. V. Shishkin, J. Leszczynski, *J. Chem. Phys.,* 2000, **113**, 5986.
[86] O. V. Shishkin, L. Gorg, P. Hobza, J. Leszczynski, *Int. J. Quantum Chem.,* 2000, **80**, 1116.
[87] S. Muñoz-Freán, M. Alcolea Palafox, V.K. Rastogi, *J. Molec. Struct.,* 2013, **1054-1055**, 32.
[88] V. I. Danilov, T. van Mourik, V. I. Poltev, *Chem. Phys. Lett.,* 2006, **429**, 255.
[89] W. Kolodziejski, J. Klinowski, *Chem. Phys. Letts.*, 1999, **303**, 183.
[90] V.E. Marquez, A. Ezzitouni, P. Russ, M.A. Siddiqui, H. Ford, Jr., R.J. Feldman, H. Mitsuya, C. George, J.J. Barchi, Jr. *J. Am. Chem. Soc.*, 1998, **120**, 2780.
[91] S. Dijkstra, J.M. Benevides, G.J. Thomas, Jr., *J. Molec. Struct.,* 1991, **242**, 283.
[92] M. Alcolea Palafox, *J. Biomolec. Struct. Dyn.*, 2014, **32** (5) 831.
[93] M.C. Alvarez-Ros, M. Alcolea Palafox, *J. Molec. Struct.,* 2013, **1047**, 358.
[94] A.A. El-Sayed, M. C. Alvarez-Ros, A. Tamara Molina, M. Alcolea Palafox, *J. Biomol. Struct. Dyn.,* 2014, in press, DOI: 10.1080/07391102.2014.909743
[95] H.-T. Ho, M.J.M. Hitchcock, *Antimicrob. Agents Chemother.,* 1989, **33** (4), 844.
[96] G.R. Painter, A.E. Aulabaugh, C.W. Andrews, *Biochem. Biophys. Res. Comm.,* 1993, **191** (3), 1166.

Table 1. The 55 optimum stable conformers calculated in AZT molecule at the following levels: by MP2/6-31G(d,p) (values in brackets), B3LYP/6-31G(d,p) (values in normal style), B3LYP/6-311++G(3df,pd) (values in *italic*), M052X/6-31G(d,p) (values in bold), M06L/aug-cc-pVDZ (values in bold and *italic*), PCM with B3LYP/6-31G** (values in quotation marks), B3LYP/6-31G(d,p) in AZT-$(H_2O)_{10}$ clusters (values in quotation marks and italic), AZT-$(H_2O)_{13}$ clusters with B3LYP/6-31G** (values in quotation marks and bold type), and AZT-$(H_2O)_{13}$ clusters with B3LYP/6-311++G(2d,p) (values in quotation marks, *italic* and bold type). Endocyclic and exocyclic torsional angles in degrees, pseudorotational angle P in degrees, dipole moment μ in Debyes, and energy increments in (kcal mol^{-1}).

Conf	χ	β	γ	ϕ	δ	ν_0	ν_1	ν_2	ν_3	ν_4	P[a]	S[b]	ν^c_{max}	μ	ΔE	ΔG
B1	[62.3] 61.5 **62.2**	[41.6] 43.5 **40.4**	[47.1] 44.2 **47.6**	[91.4] 99.1 **107.0**	[91.2] 94.5 **92.0**	[-14.9] -11.8 **-13.93**	[-5.1] -5.2 **-5.76**	[21.5] 18.6 **21.38**	[-30.7] -25.7 **-29.99**	[28.9] 24.0 **27.99**	[45.8] 44.5 **45.1**	[$_4$E] $^3_4$T $_4$E	[31.1] 26.1 **30.3**	[5.64] 4.95 **5.20**	[0][d] 0.024 **0.109**	0[f] 0.295 **0.311**
B2	[61.9] 61.3 **62.0** **"67.6"**	[41.9] 43.8 **40.8** **"84.8"**	[45.8] 43.4 **46.9** **"50.5"**	[161.9] 113.1 **110.8** **"111.0"**	[94.0] 94.4 **92.2** **"83.7"**	[-14.6] -10.6 **-13.56** **"-14.40"**	[-5.5] -6.9 **-5.97** **"-7.97"**	[21.8] 20.1 **21.37** **"25.42"**	[-30.9] -26.6 **-29.76** **"-34.25"**	[28.8] 23.8 **27.61** **"30.84"**	[46.3] 41.3 **44.6** "**42.4**"	[$_4$E] $^3_4$T $^3_4$**T** "$^3_4$**T**"	[31.2] 26.7 **30.0** "**34.4**"	[5.60] 5.04 **5.21** **"9.73"**	[0.047] 0[e] **0**[p] "**1.943**"	0[f] **0**[q] **"2.195"**
B3	[62.3] 61.7 ***62.9***	[41.5] 42.9 ***36.2***	[47.5] 45.0 ***49.0***	[-53.7] -53.2 ***-54.5***	[86.5] 88.9 ***85.9***	[-15.3] -12.2 ***-13.89***	[-4.8] -5.0 ***-5.75***	[21.3] 18.6 ***21.42***	[-30.7] -25.9 ***-29.89***	[29.1] 24.3 ***27.79***	[47.0] 45.1 ***44.9***	[$_4$E] $_4$E "$^3_4$***T***"	[31.2] 26.3 ***30.3***	[5.61] 4.33 ***4.28***	[0.686] 1.512 ***0***[r]	1.895 ***0***[s]
B4	[65.6] 68.2	[-58.1] -58.4	[178.1] 179.0	[87.0] 98.9	[95.3] 94.1	[-5.8] -5.4	[-1.4] -12.2	[22.9] 23.5	[-6.8] -27.1	[20.9] 20.8	[29.6] 29.6	$^3_4$T	[25.2] 27.0	[4.50] 3.94	[2.447] 2.177	1.644
B5	67.9	170.6	-62.5	152.6	101.1	-0.7	-13.4	20.9	-21.9	14.6	20.2	^{3}E	22.4	2.68	3.313	3.238
B6	67.7	-59.5	179.3	-54.1	88.4	-6.1	-11.4	22.9	-26.9	21.2	31.2	$^3_4$T	26.9	3.44	3.338	3.156
B7	71.2	50.7	-75.1	75.8	80.9	-13.8	-10.0	27.8	-36.6	32.0	40.2	$^3_4$T	36.4	3.74	3.941	3.784
B8	67.3	66.7	-176.2	97.4	93.0	-3.7	-12.9	23.0	-25.7	18.9	26.7	^{3}E	25.8	4.11	4.461	3.828
B9	67.5	-172.5	-171.1	99.0	91.6	-5.8	-12.1	23.7	-27.7	21.5	30.4	$^3_4$T	27.5	1.98	4.493	3.796
B10	78.0	178.9	50.4	106.6	84.8	-9.2	-13.0	28.2	-34.3	27.7	33.8	$^3_4$T	33.9	4.13	5.127	4.298
B11	68.2	-74.5	-58.8	153.1	101.6	-0.11	-13.34	20.38	-20.94	13.53	18.7	^{3}E	21.5	4.50	3.271	3.199
C1	[-126.9] -128.1 *-127.6* **-129.2** "-125.8"	[176.4] 176.5 *179.4* **177.4** "176.9"	[49.1] 50.2 *51.0* **50.0** "50.1"	[63.8] 70.9 *74.2* **64.7** "77.0"	[144.5] 140.0 *136.6* **143.4** "144.6"	[-21.5] -19.4 *-21.73* **-21.23** "-14.74"	[34.7] 31.6 *32.01* **33.84** "29.70"	[-34.1] -31.1 *-29.82* **-33.06** "-32.56"	[22.5] 20.6 *17.96* **21.71** "24.78"	[-0.1] -0.9 *2.26* **-0.44** "-6.50"	[162.6] 162.9 *157.5* **162.1** "172.5"	[^{2}E] ^{2}E ^{2}*E* ^{2}**E** "$^2_3$T"	[35.8] 32.5 *32.3* **34.7** "32.8"	[7.79] 6.88 *6.92* **7.16** "8.88"	[0.627] 1.556 *0.206* **1.028** "0"[g]	1.468 **1.114** "0.473"
C2	[-133.4] -129.1 *-117.5* **-130.3** "-143.1" "**-65.7**" "**-90.3**"	[69.4] 68.8 *68.6* **68.8** "92.3" "**85.0**" "**76.7**"	[61.9] 61.9 *58.2* **63.1** "59.7" "**60.3**" "**52.1**"	[85.0] 95.9 *91.3* **92.9** "102.4" "**115.0**" "**74.4**"	[85.1] 87.3 *85.46* **86.7** "85.0" "**92.6**" "**137.0**"	[-5.3] -7.55 *-18.52* **-6.34** "-3.28" "**16.55**" "**-29.75**"	[-17.7] -14.00 *-3.96* **-16.03** "-18.80" "**-33.08**" "**37.46**"	[32.3] 28.32 *22.65* **30.41** "31.93" "**36.40**" "**-31.60**"	[-36.1] -33.32 *-33.93* **-34.82** "-34.50" "**-27.16**" "**15.07**"	[26.4] 26.17 *33.49* **26.34** "24.17" "**7.02**" "**9.06**"	[26.8] 31.3 *49.6* **28.8** "23.7" "**352.2**" "**147.8**"	[^{3}E] $^3_4$T $_4$*E* $^3_4$**T** "^{3}E "$^3_2$**T**" "$^2_1$**T**"	[36.1] 33.2 *35.0* **34.7** "34.9" "**36.7**" "**37.3**"	[3.76] 2.82 *2.62* **3.21** "4.97" "**4.70**" "**5.77**"	[0.690] 1.050 *0*[h] **1.057** "0.840"[j] "**0**" [k] "**11.906**"	0.729 **0.540** "1.940" "**0**" [l] "**10.570**"

	"*-78.9*"	"***88.5***"	"***63.4***"	"***91.7***"	"***96.0***"	"***17.17***"	"*-29.92*"	"***31.01***"	"*-21.37*"	"***2.87***"	"***346.5***"	"$_2$***E***"	"*31.9*"	"***5.95***"	"*0*"[o]	
C3	[-130.9] "*-103.7*" "**-101.9**" "***-94.9***"	[68.6] "*77.3*" "**78.4**" "***83.1***"	[60.5] "*50.0*" "**52.2**" "***52.9***"	[161.2] "*166.0*" "**179.6**" "***169.9***"	[89.2] "*136.9*" "**138.7**" "***138.8***"	[-6.3] "*-31.53*" "**-33.09**" "*-27.91*"	[-16.8] "*38.08*" "**39.69**" "***36.13***"	[31.6] "*-30.53*" "**-31.64**" "*-30.77*"	[-35.9] "*12.80*" "**13.27**" "***15.25***"	[26.8] "*11.65*" "**12.26**" "***7.80***"	[28.3] "*143.9*" "**143.6**" "***149.1***"	[$^3_4$T] "$^2_1$*T* "$^2_1$**T**" "$^2_1$***T***"	[28.3] "*37.8*" "**39.3**" "***35.8***"	[3.76] "*9.43*" "**6.31**" "***7.52***"	[0.941] "*0*"[m] "**2.743**" "***7.724***"	"*0*"[n] "**1.729**"
C4	[-125.1] -126.0 *-124.9* "-125.2"	[175.9] 175.9 *178.6* "176.1"	[48.6] 49.5 *50.4* "50.3"	[-176.9] 173.9 *171.9* "166.9"	[149.5] 145.1 *141.3* "148.7"	[-20.6] -18.1 *-20.67* "-14.24"	[34.7] 31.4 *32.10* "29.99"	[-34.8] -31.9 *-30.75* "-33.30"	[23.7] 22.2 *19.49* "25.79"	[-2.0] -2.6 *0.68* "-7.38"	[164.6] 165.8 160.3 "173.8"	[^{2}E] ^{2}E ^{2}E "$^2_3$T"	[35.8] 32.9 32.7 "33.5"	[7.85] 6.47 *6.60* "8.57"	[0.951] 1.845 *0.527* "0.048"	1.675 "0.334"
C5	[-127.5] -128.7 "-125.2"	[-93.5] -90.5 "-88.4"	[51.7] 52.9 "54.2"	[63.1] 69.2 "74.7"	[145.7] 141.2 "144.3"	[-21.2] -18.9 "-15.58"	[34.7] 31.6 "30.08"	[-34.6] -31.6 "-32.42"	[23.1] 21.4 "24.15"	[-1.4] -1.7 "-5.56"	[141.7] 164.3 "170.9"	[$^2_1$T] ^{2}E "^{2}E"	[44.1] 32.8 "32.8"	[7.70] 6.44 "8.64"	[0.997] 2.861 "0.321"	2.774 "0.224"
C6	[-133.9] -129.5	[69.7] 68.8	[62.2] 62.4	[-51.4] -50.3	[80.1] 81.6	[-5.03] -7.4	[-18.13] -14.1	[32.58] 28.3	[-36.30] -33.2	[26.29] 25.9	[26.3] 30.9	[^{3}E] $^3_4$T	[36.3] 32.9	[3.70] 2.64	[1.110] 2.202	1.826
C7	-127.0 "-118.8"	-55.3 "-65.9"	178.5 "-174.5"	91.6 "95.7"	84.8 "84.6"	-23.8 "-25.64"	0.2 "1.94"	21.2 "20.09"	-35.6 "-35.56"	37.9 "38.90"	56.3 "58.8"	$_4$E	38.1 "38.8"	2.33 "3.20"	3.099 "1.291"[j]	1.769 "1.561"
C8	-126.0	-89.1	52.4	178.0	146.8	-17.42	31.44	-32.66	23.37	-3.83	167.8	^{2}E	33.4	6.28	3.109	3.153
C9	[-125.8] -126.5	[177.7] 177.9	[47.4] 49.1	[-59.4] -60.4	[139.5] 134.2	[-16.3] -15.5	[30.2] 27.9	[-31.8] -28.8	[23.0] 20.5	[-4.4] -3.3	[168.9] 167.5	^{2}E	[32.4] 29.5	[7.55] 6.88	[1.506] 3.175	2.949
C10	[-146.7] -131.1	[-32.1] -50.7	[164.6] 174.0	[65.0] 74.1	[155.7] 133.9	[-11.36] -31.3	[30.24] 37.3	[-36.60] -29.1	[30.80] 11.7	[-12.44] 12.2	[180.8] 142.4	$^2_3$T $^2_1$T	[36.6] 36.8	[4.63] 3.74	[3.202] 3.319	2.177
C11	-128.4	-48.8	172.1	175.2	145.2	-24.7	35.7	-34.7	19.1	3.4	156.0	^{2}E	37.6	3.83	3.596	2.692
C12	-138.5 "-126.8"	-69.7 "-69.5"	-63.2 "-64.6"	75.2 "78.0"	137.9 "139.5"	-28.4 "-27.77"	37.4 "37.45"	-31.7 "-32.52"	16.1 "17.33"	7.6 "6.38"	149.6 "151.5"	$^2_1$T	36.8 "37.0"	4.37 "5.66"	3.696 "1.655"[j]	2.648 "2.016"
C13	[-133.3] -131.9	[-75.0] -73.9	[-65.4] -63.8	[-176.3] 174.0	[150.4] 138.0	[-25.4] -30.15	[38.7] 37.44	[-36.5] -30.18	[22.7] 13.51	[1.5] 10.37	[159.1] 145.2	[^{2}E] $^2_1$T	[39.1] 36.7	[5.22] 3.96	[3.953] 3.739	2.685
C14	-131.3 "-125.9"	-75.6 "-73.5"	-57.8 "-61.1"	168.2 "164.5"	113.8 "112.7"	-39.3 "-39.77"	32.5 "32.27"	-14.4 "-13.55"	-8.1 "-9.19"	29.8 "30.67"	11.9 "110.4"	^{3}E "$^0_1$T"	38.5 "38.8"	3.24 "4.03"	3.916 "1.843"[j]	2.949 "2.688"
C15	-126.8	-56.1	178.8	-50.7	79.1	-24.9	1.2	20.5	-35.5	38.5	57.8	$_4$E	38.5	2.67	4.010	3.175
C16	-140.7 "-121.5"	-176.1 "174.4"	-65.9 "-69.9"	78.3 "77.5"	140.8 "139.3"	-26.8 "-28.35"	37.0 "37.72"	-32.7 "-32.47"	18.1 "16.95"	5.3 "6.97"	153.1 "150.7"	^{2}E "$^2_1$T"	36.7 "37.2"	5.74 "7.55"	4.223 "2.188"[j]	2.861 "3.004"
C17	"-117.7"	"179.6"	"-173.9"	"98.8"	"84.1"	"-26.53"	"2.93"	"19.38"	"-35.40"	"39.31"	"60.2"	"$_4$E"	"39.0"	"5.95"	"2.254"[j]	"2.595"
C18	[-122.2] -124.7 "-116.6"	[-178.7] 179.9 "174.5"	[-59.0] -61.0 "-64.5"	[157.4] 152.8 "150.9"	[90.5] 91.5 "90.0"	[-16.2] -27.7 "-27.08"	[-7.2] 5.9 "4.55"	[25.7] 15.5 "17.24"	[-35.8] -32.1 "-33.52"	[33.2] 38.1 "38.4"	[44.6] 65.3 "62.9"	[$^3_4$T] $^0_4$T "$_4$E"	[36.1] 37.1 "37.8"	[4.56] 3.81 "4.60"	[4.894] 4.336 "2.319"	3.213 "1.158"
C19	-126.5	-90.6	51.7	-64.3	136.1	-15.04	28.17	-29.79	21.73	-4.39	169.4	^{2}E	30.3	6.62	4.346	4.261
C20	[-121.6]	[-75.9]	[-55.6]	[156.1]	[90.6]	[-15.8]	[-7.2]	[25.2]	[-35.2]	[32.5]	[135.5]	[$^2_1$T]	[35.4]	[3.80]	[4.957]	4.819

	-125.1	-75.1	-56.6	150.6	93.3	-30.8	10.7	11.1	-29.5	38.4	72.2	$^{0}_{4}$T	37.2	2.56	4.116	
C21	-144.5 “116.7”	76.6 “81.4”	-74.4 “-72.4”	71.5 “90.2”	138.4 “86.4”	-27.9 “-25.80”	37.3 “2.65”	-32.2 “19.07”	16.9 “-34.53”	6.8 “38.32”	150.9 “59.9”	$^{2}_{1}$T “$_{4}$E”	36.8 “38.0”	4.44 “4.56”	5.265 “3.020”[j]	2.692 “2.654”
C22	-134.0 “-117.9”	67.0 “68.3”	-177.3 “-178.2”	89.8 “98.2”	83.2 “84.4”	-27.2 “-25.94”	3.9 “2.53”	18.1 “19.42”	-34.6 “-35.08”	39.3 “38.71”	62.0 “59.7”	$_{4}$E	38.6 “38.5”	3.75 “5.23”	5.415 “1.891”[j]	2.937 “1.995”
C23	-136.1	-70.6	-63.5	-69.1	135.0	-22.4	33.1	-30.5	18.3	2.4	157.1	^{2}E	33.1	4.49	5.723	4.462
A1	[-161.3]	[175.8]	[47.3]	[163.8]	[83.2]	[3.74]	[-27.38]	[38.75]	[-37.69]	[21.52]	[13.3]	[^{3}E]	[39.8]	[6.38]	[0.999]	
A2	[-162.3] -159.4	[178.9] 179.8	[51.1] 52.0	[-50.5] - 49.0	[76.4] 79.1	[4.12] 2.6	[-27.14] -23.3	[38.12] 33.4	[-36.82] -32.7	[20.82] 19.2	[12.7] 14.2	^{3}E	[39.1] 34.4	[6.32] 5.52	[1.386] 2.416	2.441
A3	[-163.3] -161.0	[-89.5] -91.1	[51.4] 53.6	[72.5] 83.2	[79.5] 83.1	[5.41] 3.9	[-28.58] -24.9	[39.46] 34.9	[-37.40] -33.6	[20.34] 19.0	[11.1] 12.5	^{3}E	[40.2] 35.8	[5.53] 4.96	[1.640] 2.008	1.851
A4	[-162.3]	[-97.7]	[49.3]	[165.5]	[82.8]	[4.6]	[-28.2]	[39.4]	[-37.8]	[20.9]	[12.1]	[^{3}E]	[40.3]	[5.74]	[2.071]	
A5	[-168.2] -163.8	[-54.1] -55.9	[176.6] 178.9	[-51.8] - 49.8	[79.5] 78.5	[7.3] -1.8	[-29.4] -20.8	[38.9] 33.7	[-35.6] -35.4	[18.1] 23.8	[20.0] 21.2	^{3}E	[41.4] 36.1	[2.0] 1.72	[2.349] 3.884	3.357
A6	[-162.7] -159.7	[-88.2] -88.7	[50.6] 51.8	[-50.6] -48.6	[74.9] 77.4	[5.2] 3.62	[-28.5] -24.83	[39.4] 34.94	[-37.5] -33.72	[20.5] 19.21	[11.3] 12.8	^{3}E	[40.2] 35.8	[5.51] 4.70	[2.395] 2.705	2.858
A7	[-162.4] -160.2 “-157.7”	[176.8] 177.1 “173.2”	[50.4] 51.6 “51.7”	[84.9] 96.8 “101.9”	[81.1] 84.6 “86.6”	[4.2] 2.9 “3.70”	[-27.1] -23.8 “-23.90”	[38.1] 33.9 “33.50”	[-36.7] -33.0 “-32.02”	[20.7] 19.33 “18.19”	[12.6] 13.8 “12.4”	^{3}E	[39.1] 34.9 “34.3”	[6.32] 5.68 “7.14”	[2.399] 1.267 “0.098”	0.929 “0”[i]
A8	[-168.8] -164.6	[-53.2] -55.2	[176.0] 178.6	[80.1] 89.6	[84.7] 84.4	[7.8] -0.6	[-29.5] -21.7	[38.8] 34.1	[-35.1] -35.1	[17.4] 22.9	[7.2] 19.3	[$^{3}_{2}$T] ^{3}E	[39.1] 36.2	[1.93] 1.87	[3.137] 2.937	2.165
A9	[-169.5] -165.0	[56.0] 53.6	[168.5] 164.2	[62.1] 69.0	[156.6] 150.1	[5.93] -0.2	[16.92] 20.1	[-31.54] -30.7	[35.85] 31.4	[-26.60] -20.1	[207.9] 18.2	[$^{4}_{3}$T] ^{3}E	[35.7] 32.3	[6.15] 5.42	[3.633] 4.141	3.922
A10	[-170.8] -167.0	[179.0] 179.1	[-62.3] -64.1	[158.1] 154.6	[91.8] 90.4	[9.9] 1.7	[-29.8] -22.4	[36.8] 32.8	[-31.8] -32.5	[14.1] 19.8	[3.1] 15.6	[$^{3}_{2}$T] ^{3}E	[36.9] 34.0	[4.83] 4.16	[3.828] 4.054	3.847
A11	[-171.0] -167.4	[-74.3] -73.3	[-58.4] -59.5	[156.4] 150.7	[92.2] 90.3	[10.93] 1.9	[-30.18] -22.3	[36.48] 32.4	[-30.95] -32.0	[12.89] 19.4	[1.4] 15.2	[$^{3}_{1}$T] ^{3}E	[36.5] 33.6	[4.83] 4.08	[3.840] 3.916	3.658
A12	-167.7	50.6	-75.4	70.8	77.5	-1.8	-22.3	36.2	-38.1	25.5	21.2	^{3}E	38.8	1.95	3.972	3.715
A13	[-175.2]	[-175.3]	[-63.7]	[65.3]	[158.6]	[0.60]	[21.37]	[-33.73]	[35.03]	[-22.65]	[199.6]	[$_{3}$E]	[35.8]	[4.91]	[4.239]	
A14	-167.7	57.5	-71.5	- 46.0	74.9	-0.5	-22.6	35.3	-36.4	23.5	19.2	^{3}E	37.4	1.82	4.461	4.248
A15	[-177.9] -172.5	[54.9] 63.9	[164.6] 175.5	[77.7] 88.4	[99.6] 88.0	[27.57] 9.4	[-36.59] -27.1	[31.39] 33.2	[-16.30] -28.6	[-6.91] 12.4	[330.4] 2.5	[$^{1}_{2}$T] $^{3}_{2}$T	[36.1] 33.2	[4.51] 4.11	[4.772] 4.706	5.384
A16	-169.8	179.1	172.8	68.1	151.3	5.22	15.75	-28.91	32.58	-24.24	207.5	$^{4}_{3}$T	32.6	5.44	4.875	4.762
A17	[-177.4]	[53.9]	[163.8]	[167.5]	[103.7]	[27.4]	[-36.3]	[30.8]	[-15.7]	[-7.2]	[149.8]	[$^{2}_{1}$T]	[35.6]	[4.63]	[5.045]	
A18	-168.3	56.4	167.4	-50.5	146.5	8.4	13.1	-27.6	32.9	-26.5	32.8	$^{3}_{4}$T	32.8	5.38	5.095	5.202
A19	[-178.5]	[173.2]	[171.8]	[77.9]	[98.6]	[26.8]	[-36.6]	[32.1]	[-17.5]	[-5.7]	[152.4]	[$^{2}_{1}$T]	[36.2]	[3.85]	[5.334]	

	-170.4	176.6	-175.4	88.1	84.1	3.85	-24.52	34.29	-32.86	18.64	12.4	^{3}E	35.1	4.20	4.959	4.105
A20	[-170.7]	[88.1]	[-71.3]	[155.0]	[63.9]	[-9.83]	[29.22]	[-36.39]	[31.66]	[-13.92]	[183.3]	$[\frac{2}{3}T]$	[36.4]	[4.01]	[5.614]	
A21	-174.5	-178.3	-65.7	-52.3	147.7	3.2	17.3	-29.5	31.9	-22.6	23.9	^{3}E	32.3	4.70	5.848	5.390

[a] Definition: $tgP = \frac{(\nu_4 + \nu_1) - (\nu_3 + \nu_0)}{2\ \nu_2(\sin(36) + \sin(72))}$ When ν_2 is negative, 180º is added to the calculated value of P, ref. [62]. [b]Notation used from ref. [77]. [c]-963.27585 a.u. at B3LYP/6-31G(d,p) level. [f]ΔG= 0 = -963.32315 a.u. [g] -963.309187 a.u. with the PCM model at the B3LYP/6-31G(d,p) level. [h]ΔE= 0 = -963.850132 a.u. at B3LYP/6-311++G(3df,pd) level. [i]ΔE= 0 = -963.356242 a.u. with the PCM model at the B3LYP/6-31G(d,p) level. [j]Saddle structure. [k]ΔE= 0 = -1956.691399 a.u. at B3LYP/6-31G(d,p) in AZT-$(H_2O)_{13}$ [l]ΔG= 0 = -1956.775749 a.u. at B3LYP/6-31G(d,p) in AZT-$(H_2O)_{13}$ [m]ΔE= 0 = -1727.438550 a.u. at B3LYP/6-31G(d,p) in AZT-$(H_2O)_{10}$ [n]ΔG= 0 = -1727.516078 a.u. at B3LYP/6-31G(d,p) in AZT-$(H_2O)_{10}$ [o]ΔE= 0 = -1957.990791 a.u. at B3LYP/6-311++G(2d,p) in AZT-$(H_2O)_{13}$ [p]ΔE= 0 = -963.163626 a.u. at the M052X/6-31G(d,p) level. [q]ΔG= 0 = -963.210334 a.u. at the M052X/6-31G(d,p) level. [r]ΔE= 0 = -963.300964 a.u. at the M06L/aug-cc-pVDZ level. [s]ΔG= 0 = -963.347194 a.u. at the M06L/aug-cc-pVDZ level.

Table 2. Global minimum in AZT determined by several authors. The exocyclic torsional angles are in degrees

conformer	level	reference	χ	γ	ϕ	β
B5	HF/6-31+G(d,p)	[39]	67.3	-62.0	146.9	
B1	BLYP/6-31+G(d,p)		70.3	-65.9	148.2	
			61.0	42.6	114.4	
	B3LYP/6-31G(d)	[38]	61.0			
C6	AM1	[14]	-107.4	70.2	-60.4	65.9
C8	x-ray molecule A	[64]	-124.4	50.9	177.6	-129.1
A17	molecule B		-173.6	173.4	176.2	90.7
C8	x-ray molecule A	[65]	-125.9(5)	49.7(5)	175.8[a]	-125.3[a]
A17	molecule B		-172.0(5)	173.7(5)	175.4[a]	112.9[a]
C8	x-ray molecule A	[66]	-125.3	50.5	176.1	
A17	molecule B		-172.3	173.4	175.8	

[a]Ref. [14].

Table 3. Comparison of the molecular geometric parameters in the four most stable conformer of AZT and dT at MP2/6-31G(d,p) level. Exocyclic torsional angles in degrees, pseudorotational angle P in degrees, dipole moment μ in Debyes, and energy increments in (kcal mol^{-1})

	Conformer	χ	β	γ	ϕ	P	ν_{max}	μ	Δ*E*
dT	C1	-128.9	176.1	50.1	62.3	163.3	37.0	7.765	0
	B1	61.4	40.1	46.4	157.2	44.5	31.1	4.697	0.132
	B2	62.4	39.6	48.7	93.6	46.9	30.4	4.710	0.221
	C2	-125.1	174.9	49.3	-175.7	165.8	36.9	8.855	0.642
AZT	B1	62.3	41.6	47.1	91.4	45.8	31.1	5.64	0
	B2	61.9	41.9	45.8	161.9	46.3	31.2	5.60	0.047
	C1	-126.9	176.4	49.1	63.8	162.6	35.8	7.79	0.627
	B3	62.3	41.5	47.5	-53.7	47.0	31.2	5.61	0.686

Table 4. Intramolecular distances (in Å) between the oxygen atoms in the isolated state and in the cluster in *anti* with 13 water molecules in conformer C1 (conformer C2 in parentheses) of dT and AZT at the B3LYP/6-31G(d,p) level.

	AZT isolated	AZT-$(H_2O)_{13}$	dT isolated	dT-$(H_2O)_{13}$		
conformer	C1 (C2)	(C2)	C1[a] (C2[b])	Fig. 7b[c]	Fig. 7e[d]	Fig. 7f[e]
O5′···O2	6.123 (6.262)	(4.306)	6.166 (6.114)	6.203	5.701	7.082
O5′···O4	6.901 (6.807)	(6.116)	6.945 (6.865)	7.034	6.178	8.680
O5′···O4′	2.909 (2.787)	(2.866)	2.917 (2.926)	2.924	2.956	3.287

[a] With χ = -129.5º, β = 176.2º, γ = 51.3º and ϕ = 62.7º. [b] With χ = -125.5º, β = 174.7º, γ = 50.3º and ϕ = -176.8º. [c] With χ= -96.5º, β = 90.7º, γ = 59.2º and ϕ = 34.2º. [d] With χ= -88.4º, β = 117.1º, γ = 51.2º and ϕ = 160.5º. [e] With χ= -131.6º, β = -74.9º, γ = 35.8º and ϕ = 165.3º.

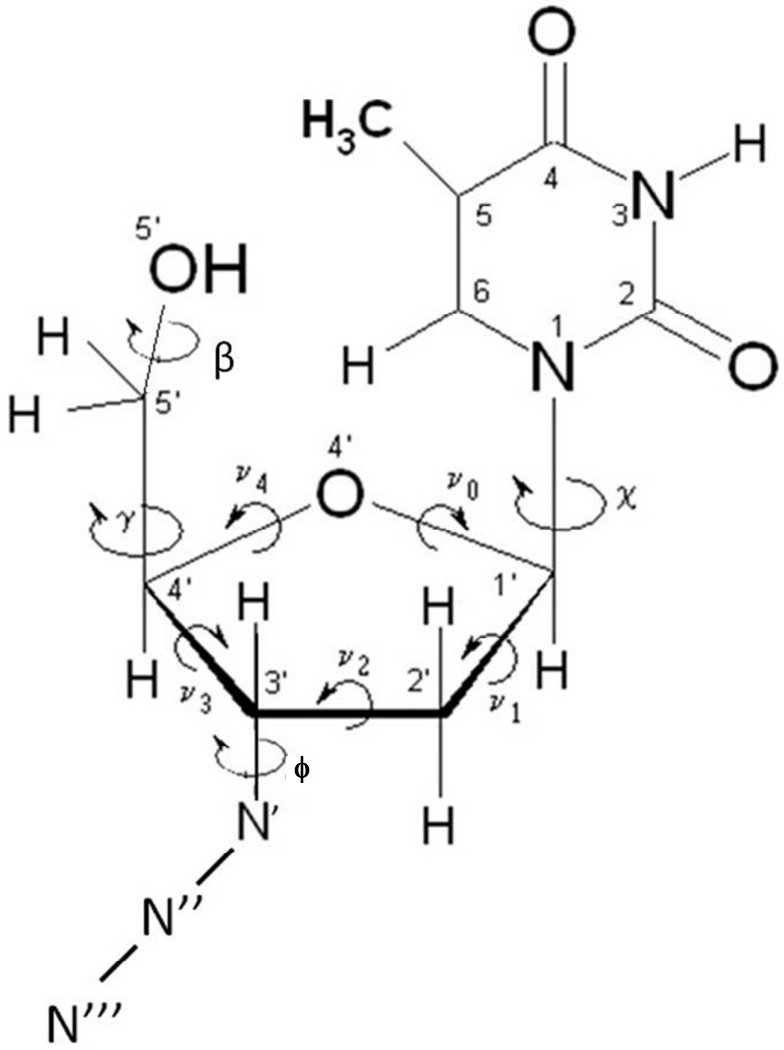

Scheme 1. Molecular structure and definition of the exocyclic and endocyclic angles in AZT.

LEGENDS OF FIGURES.

Fig. 1. Three types of conformers determined in AZT corresponding to the three ranges of rotation of χ with β and γ ~ 60º.

Fig. 2. Molecular structure of the twelve best conformers selected for each rotation angle χ determined in AZT. The values of the most important conformational parameters and the strongest intramolecular H-bonds distances are also included at the B3LYP/6-31G(d,p) and MP2/6-31G(d,p) (values in brackets) levels.

Fig. 3. Distribution of the 55 optimum conformers calculated in AZT according to their phase angle of pseudorotation P and their: (a) relative electronic energy ΔE + ZPE correction; (b) relative Gibbs energy ΔG; and (c) puckering amplitude. ν_{max}. The most stable conformers of each type are pointed.

Fig. 4. Distribution of the 55 optimum stable calculated conformers in AZT according to the values of the six exocyclic torsional angles: χ, β, γ, ϕ and δ versus the pseudorotational phase angle P.

Fig. 5. Relative energies of the 55 optimum stable conformers according to the values of the exocyclic torsional angles: χ, β, γ and ϕ.

Fig. 6. Distribution of the optimized conformers according to the values of the exocyclic torsional angles γ, χ and β.

Fig. 7. Differences in the water distribution of the cluster with the first hydration shell of AZT and dT with 13 H_2O at the B3LYP/6-31G(d,p) level. The most important calculated intermolecular H-bonds (in Å) with water molecules are included in the figure. The total energy + ZPE (in a.u.) is shown in the bottom of each cluster. The value in parentheses corresponds to the Gibbs Free energy (in a.u.).

Fig. 8. Molecular structure in the global minimum of ATP.

Fig. 9. Simulation in the isolated state of the first phosphorylation step of AZT and dT with ATP. (a) The interaction of ATP with AZT produces a rotation of the H5′ hydrogen to a β angle of ca. 180º appropriate for the phosphorylation. (b) The interaction of ATP with AZT also produces a rotation of the H5′ hydrogen. (c-d) An inadequate orientation of the ATP-AZT interaction lead to a rotation of H5′ but oriented in the inadequate phosphorylation on P2 phosphorous.

Fig. 10. Simulation of the ATP-AZT interaction but including three Na atoms around the phosphate groups.

Fig. 11. Interaction of the ATP molecule with the optimum cluster of hydrated: (a) dT nucleoside, and (b) AZT nucleosides in the simulation of the first phosphorylation step. In dT a proton transfer occurs through the water molecules. In AZT this interaction is not enough strong to rotate the -O5′H group.

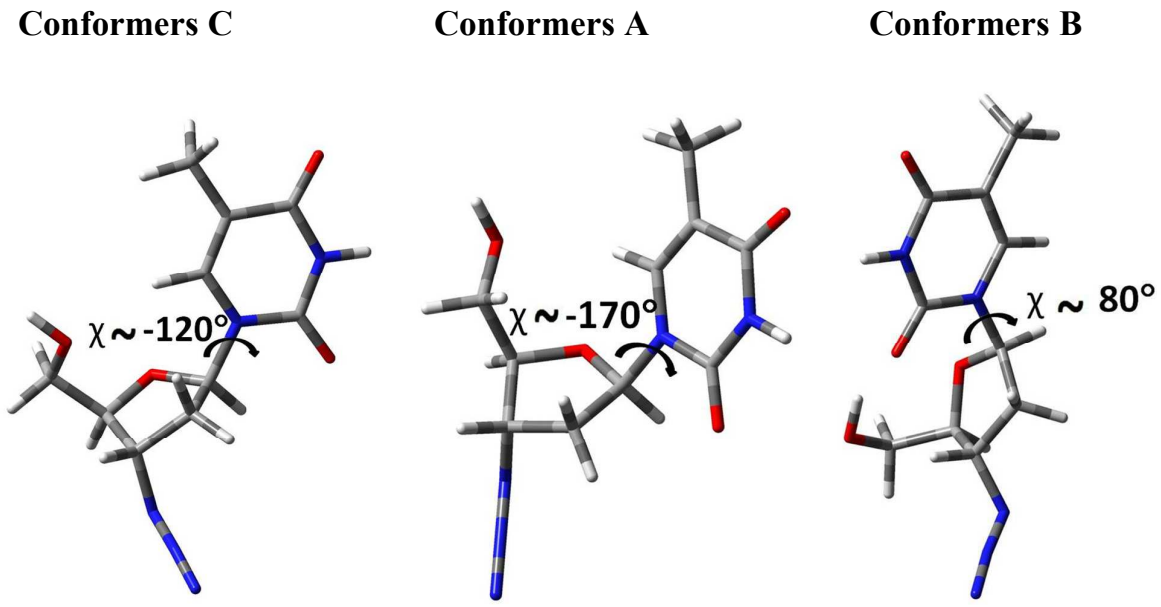

(Fig. 1)

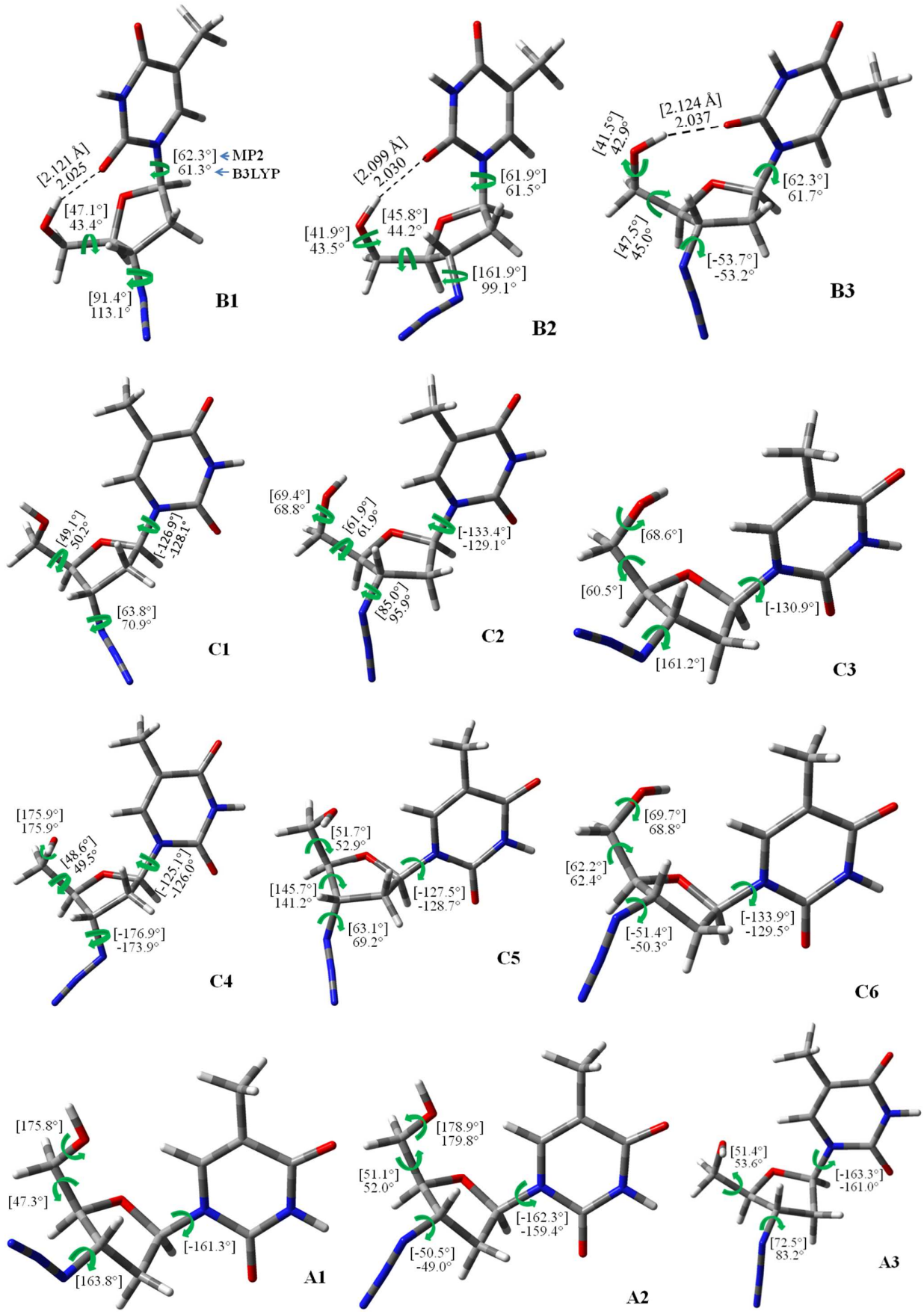

(Fig. 2)

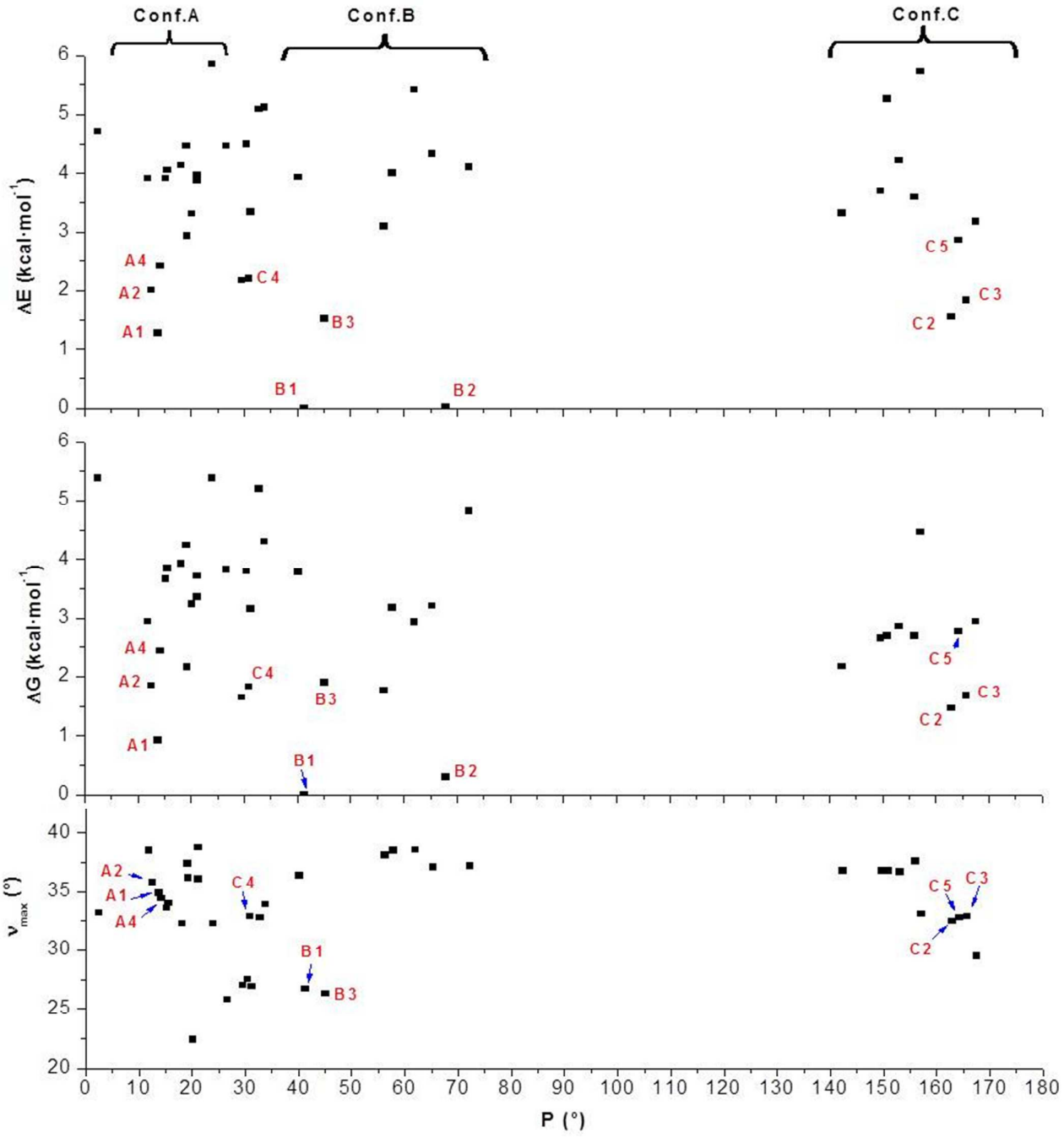

(Fig. 3)

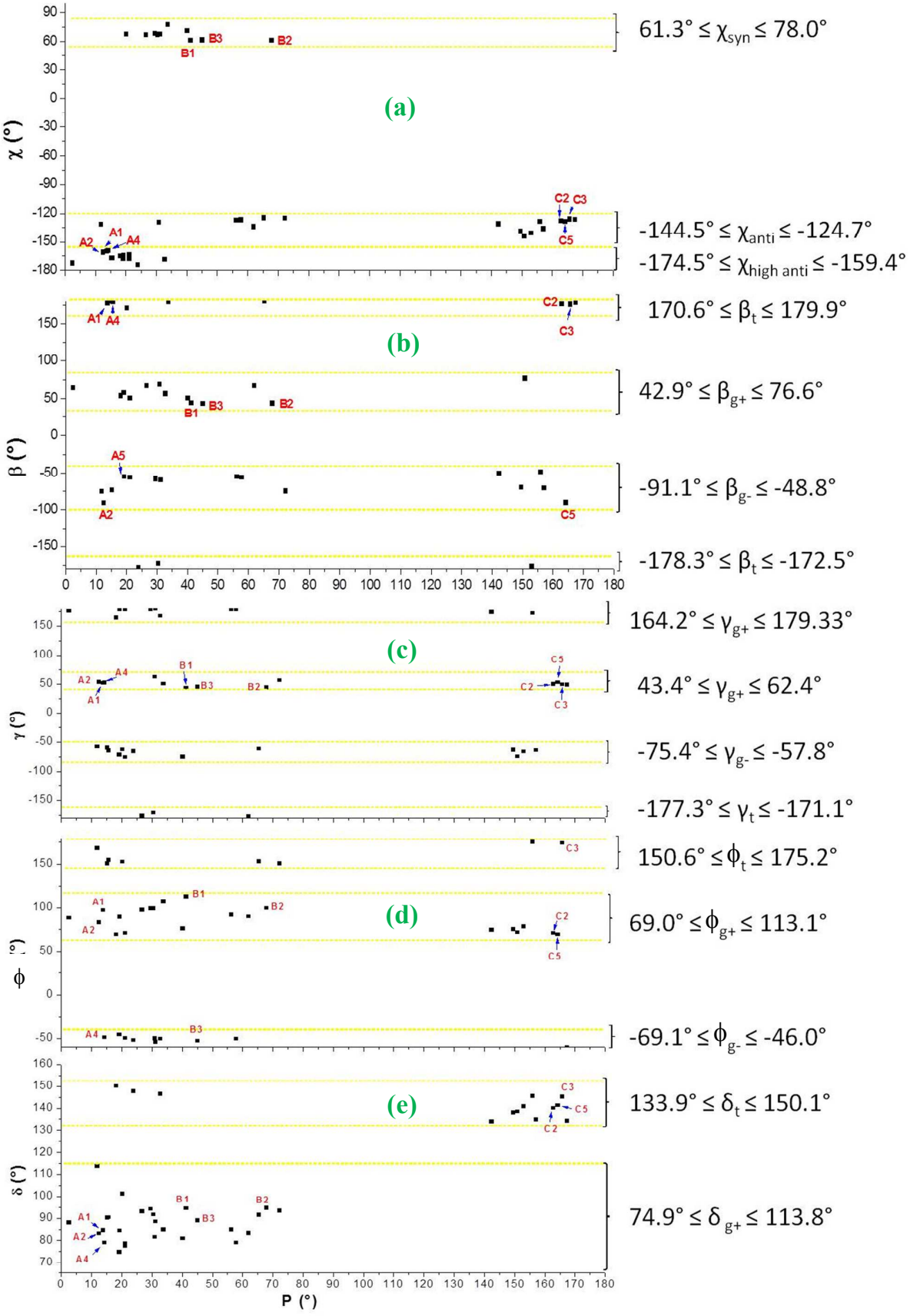

(Fig.4)

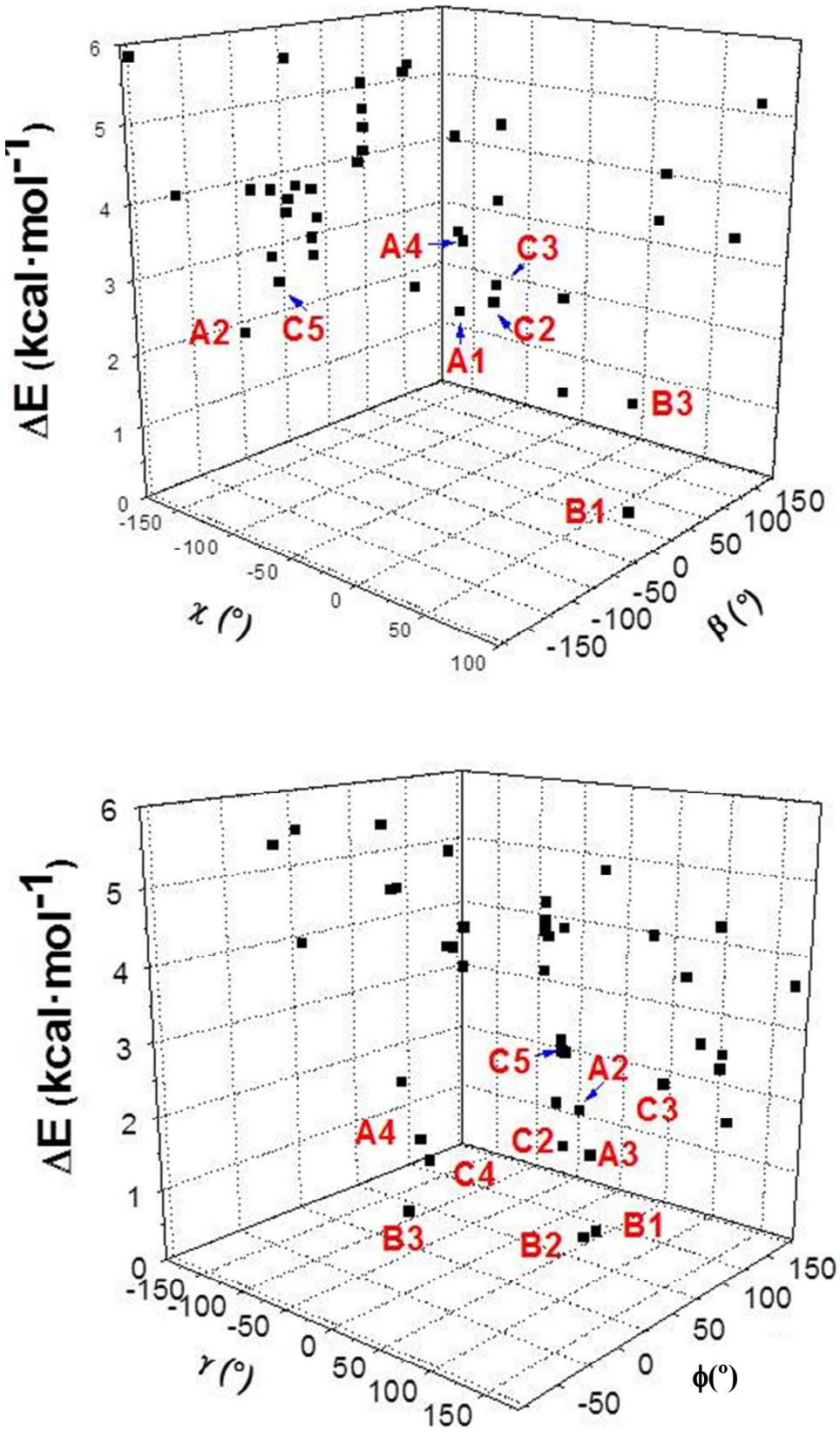

(Fig. 5)

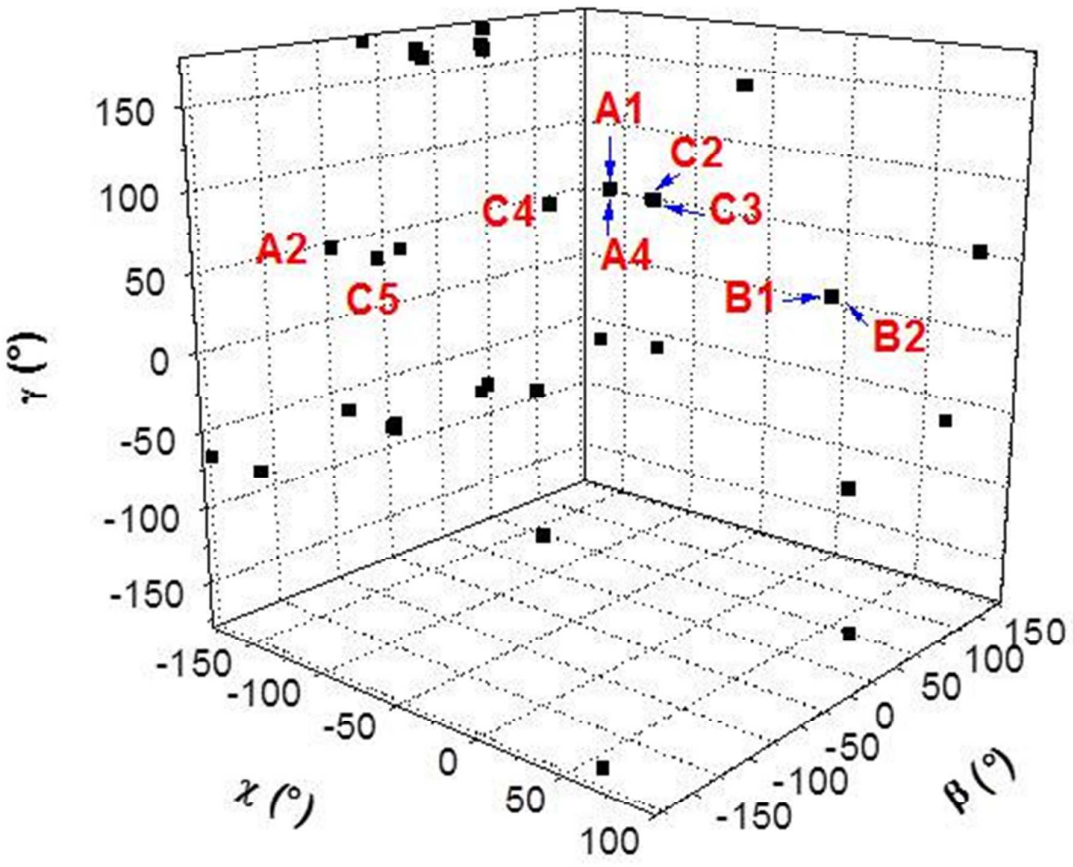

(Fig.6)

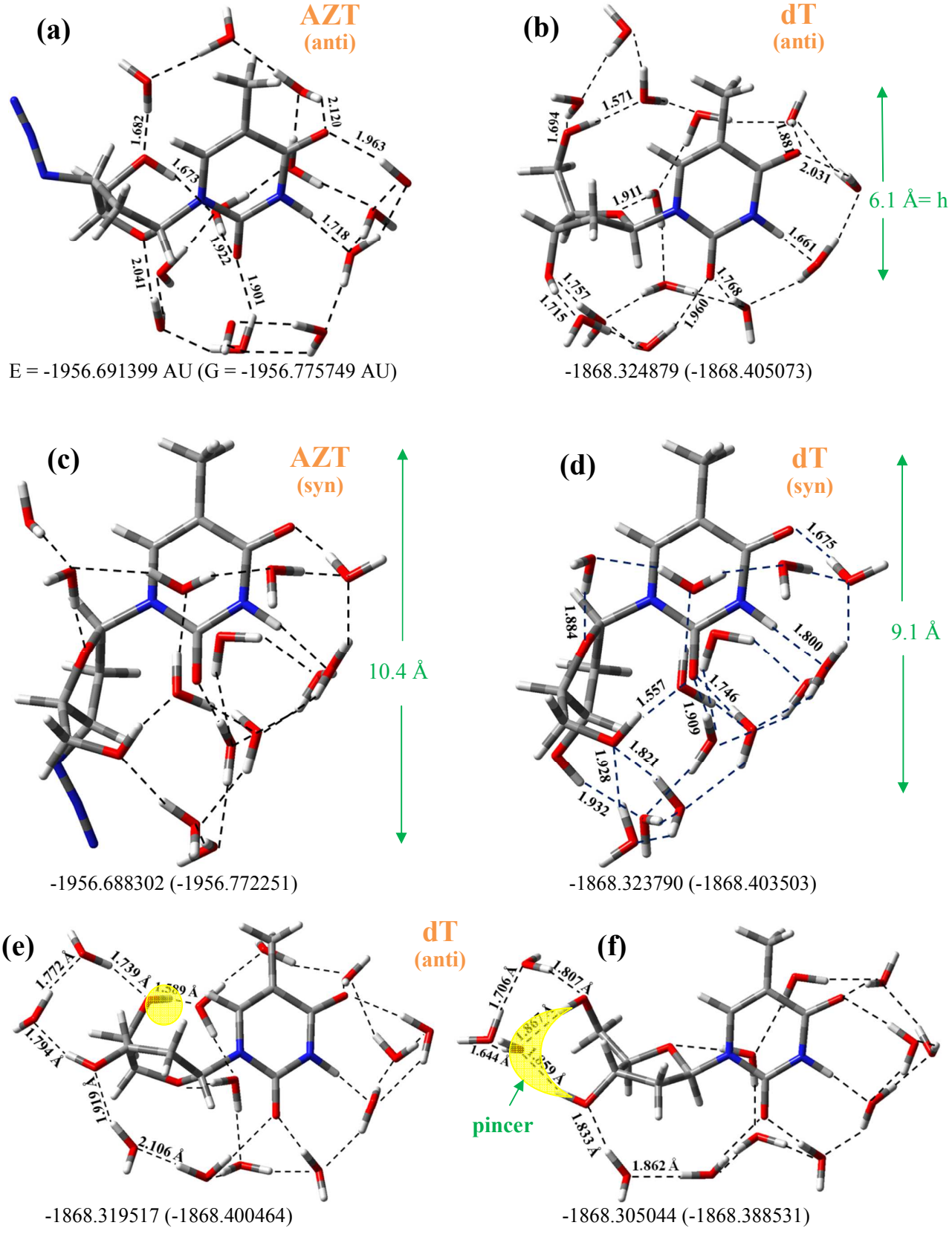

(Fig. 7)

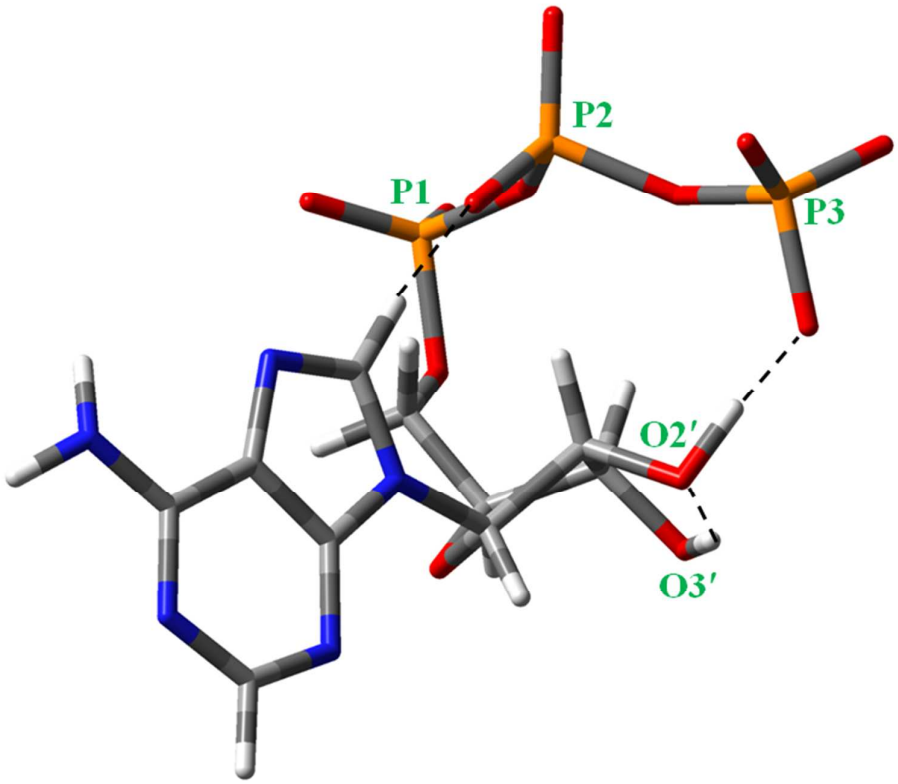

(Fig. 8)

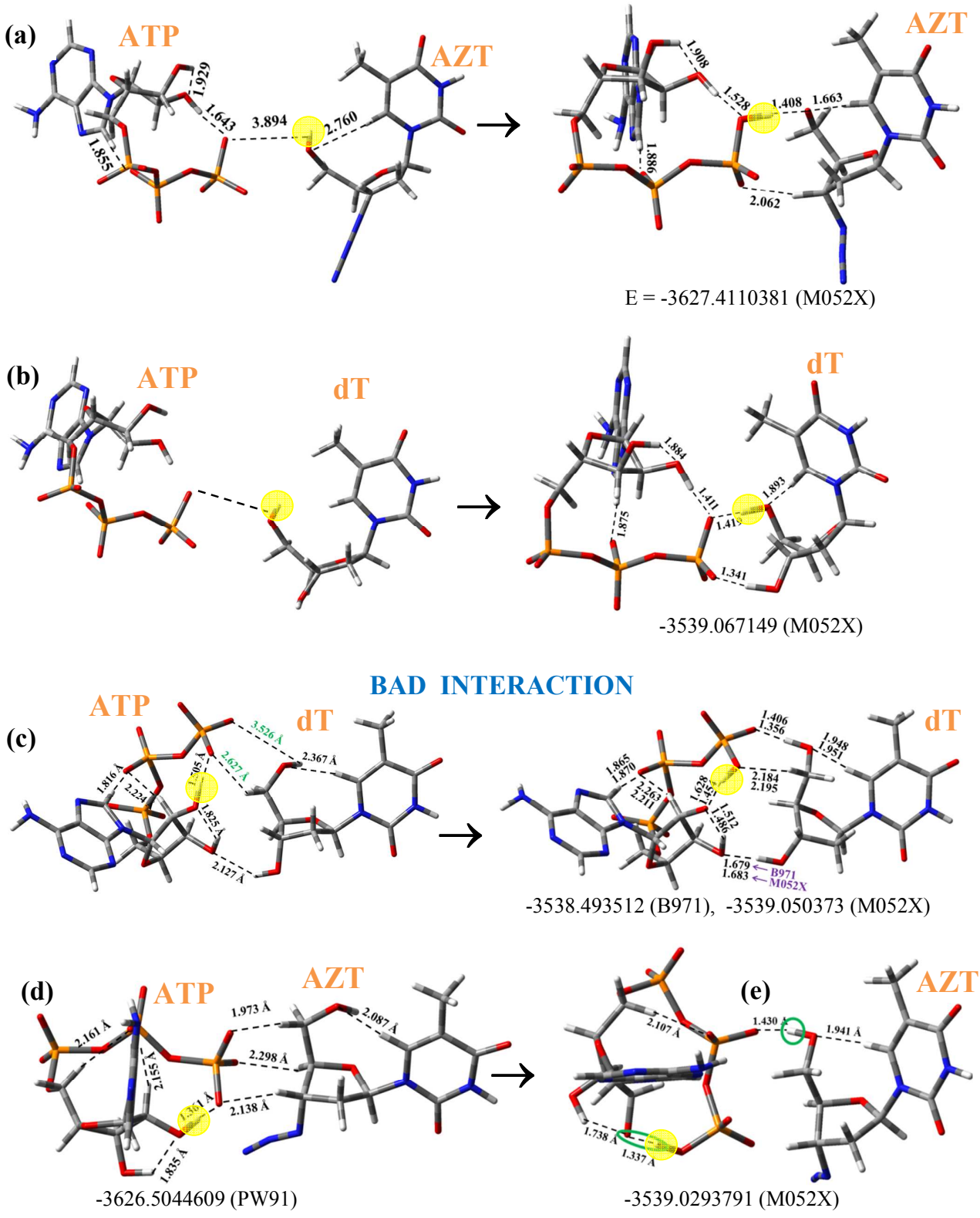

(Fig. 9)

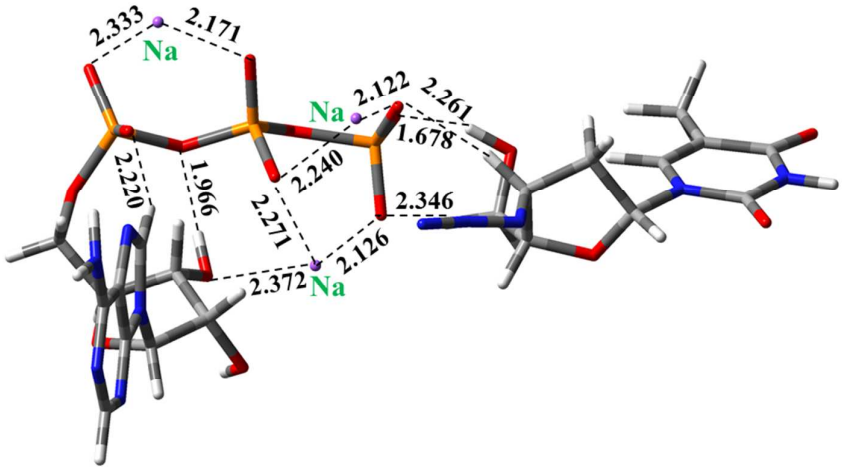

-4114.851162 (M052X)

(Fig. 10)

(a) Phosphorylation of dT:

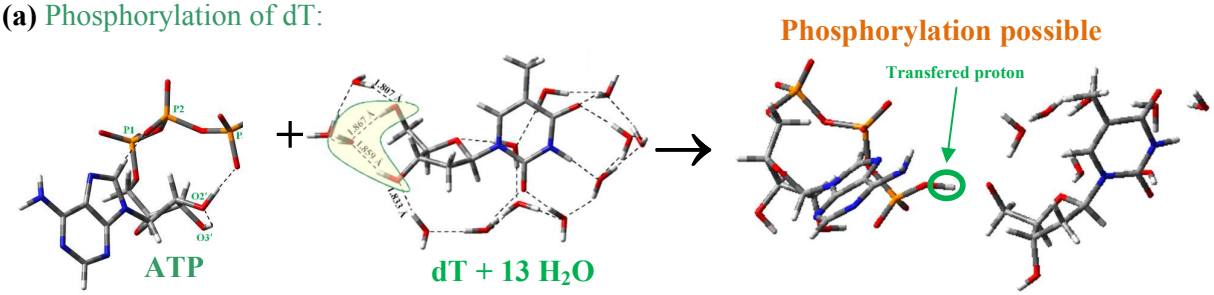

(b) Phosphorylation of AZT:

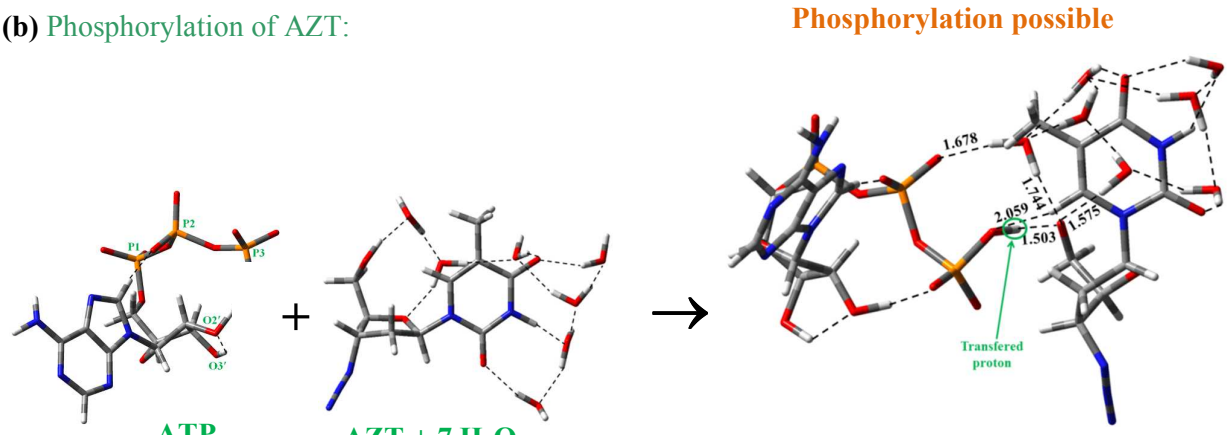

-4162.525902 (M052X)

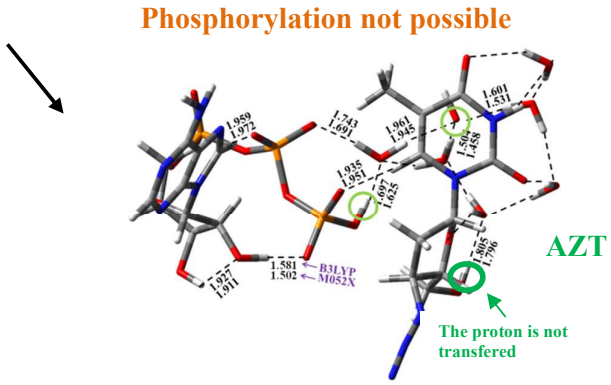

-4162.896952 (B3LYP), -4162.527790 (M052X)

(Fig. 11)